Chapter 1

Mathematical modelling

This book concerns the application of mathematics to problems in the physical sciences, and particularly to problems which arise in the study of the environment. Much of the environment consists of fluid — the atmosphere, the ocean — and even those parts which are solid may deform in a fluid-like way — ice sheets, glaciers, the Earth's mantle; as a consequence, one way into the study of the environment is through the study of fluid dynamics, although we shall not follow that approach here. Rather, we shall approach the study of environmental problems as applied mathematicians, where the emphasis is on building a suitable mathematical model and solving it, and in this introductory chapter, we set out the stall of techniques and attitudes on which the subsequent chapters are based.

There are two particular points of view which we can bring to bear on the mathematical models which describe the phenomena which concern us: these are the dynamical systems approach, or equivalently the bifurcation theory approach; and the perturbation theory approach. Each has its place in different contexts, and sometimes they overlap.

The bifurcation theory approach is most usually (but not always) brought to bear on problems which have some kind of (perhaps complicated) time-dependent behaviour. The idea is that we seek to understand the observations through the understanding of a number of simpler problems, which arise successively through bifurcations in the mathematical model, as some critical parameter is changed. A classic example of this approach is in the study of the origin of chaos in the Lorenz equations, or the onset of complicated forms of thermal convection in fluids.

In its simplest form (e. g., in weakly nonlinear stability theory) the perturbative approach is similar in method to the bifurcational one; however, the ethos is rather different. Rather than try and approach the desired solution behaviour through a sequence of simpler behaviours, we try and break down the solution by making approximations, which (with luck) are in fact realistic. In real problems, such approximations are readily available, and part of the art of the applied mathematician is having the facility of being able to judge how to make the right approximations. In this book, we follow the perturbative approach. It has the disadvantage of being harder, but it is able to get closer to a description of how realistic systems may actually behave.

1.1 Conservation laws and constitutive laws

The basic building blocks of continuous mathematical models are conservation laws. The continuum assumption adopts the view that the physical medium of concern may be considered continuous, whether it be a porous medium (for example, sand on a beach) or a fluid flow. The continuum hypothesis works whenever the length or time scales of interest are (much) larger than the corresponding microscale. For example, the formation of dunes in a desert (length scale hundreds of metres) can be modelled as a continuous process, since the microscale (sand grain size) is much smaller than the macroscale (dune length). Equally, the modelling of large animal populations or of snow avalanches treats the corresponding media as continuous.

Conservation laws arise as mathematical equations which represent the idea that certain quantities are conserved — for example, mass, momentum (via Newton's law) and energy. More generally, a conservation law refers to an equation which relates the increase or decrease of a quantity to terms representing supply or destruction.

In a continuous medium, the typical form of a conservation law is as follows:

$$\frac{\partial \phi}{\partial t} + \boldsymbol{\nabla}.\mathbf{f} = S. \tag{1.1}$$

In this equation, ϕ is the quantity being 'conserved' (expressed as amount per unit volume of medium, i. e., as a density; $\mathbf{f}$ is the 'flux', representing transport of ϕ within the medium, and S represents source ($S > 0$) or sink ($S < 0$) terms. Derivation of the point form (1.1) follows from the integral statement

$$\frac{d}{dt}\int_V \phi \, dV = -\int_{\partial V} \mathbf{f}.\mathbf{n} \, dS + \int_V S \, dV, \tag{1.2}$$

after application of the divergence theorem (which requires $\mathbf{f}$ to be continuously differentiable), and by then equating integrands, on the basis that they are continuous and V is arbitrary. Derivation of (1.1) thus requires ϕ and $\mathbf{f}$ to be continuously differentiable, and S to be continuous.

Two basic types of transport are advection (the medium moves at velocity $\mathbf{u}$, so there is an advective flux $\phi\mathbf{u}$) and diffusion, or other gradient-driven transport (such as chemotaxis). One can thus write

$$\mathbf{f} = \phi\mathbf{u} + \mathbf{J}, \tag{1.3}$$

where $\mathbf{J}$ might represent diffusive transport, for example.

Invariably, conservation laws contain more terms than equations. Here, for example, we have one scalar equation for ϕ, but other quantities $\mathbf{J}$ and S are present as well, and equations for these must be provided. Typically, these take the form of constitutive laws, and are usually based on experimental measurement. For example, diffusive transport is represented by the assumption

$$\mathbf{J} = -D\boldsymbol{\nabla}\phi, \tag{1.4}$$

where D is a diffusion coefficient. In the heat equation, this is known as Fourier's law, and the heat equation itself takes the familiar form

$$\frac{\partial}{\partial t}(\rho c_p T) + \boldsymbol{\nabla}.(\rho c_p T \mathbf{u}) = \boldsymbol{\nabla}.(k\boldsymbol{\nabla}T) + Q, \tag{1.5}$$

where Q represents any internal heat source or sink.

1.2 Non-dimensionalisation

Putting a mathematical model into non-dimensional form is fundamental. It allows us to identify the relative size of terms through the presence of dimensionless parameters. Although technically trivial, there is a certain art to the process of non-dimensionalisation, and the associated concept of scaling. We illustrate some of the precepts by consideration of the heat equation, (1.5). We write it in the form (assuming density ρ and specific heat c_p are constant)

$$\frac{\partial T}{\partial t} + \mathbf{u}.\boldsymbol{\nabla}T = \kappa\nabla^2 T + H, \tag{1.6}$$

where $H = Q/\rho c_p$. We have taken $\boldsymbol{\nabla}.\mathbf{u} = 0$, which follows from the conservation of mass equation

$$\frac{\partial \rho}{\partial t} + \boldsymbol{\nabla}.(\rho\mathbf{u}) = 0, \tag{1.7}$$

together with the supposition of incompressibility in the form $\rho =$ constant.

Suppose we are to solve (1.6) in a domain D of linear magnitude l, on the boundary of which we prescribe

$$T = T_B \ \text{ on } \ \partial D, \tag{1.8}$$

where T_B is constant. We also have an initial condition

$$T = T_0(\mathbf{x}) \ \text{ in } \ D, \quad t = 0, \tag{1.9}$$

and we suppose $\mathbf{u}$ is given, of order U.

We can make the variables dimensionless in the following way:

$$\mathbf{x} = l\mathbf{x}^*, \quad \mathbf{u} = U\mathbf{u}^*, \quad t = t_c t^*, \quad T = T_B + (\Delta T)T^*. \tag{1.10}$$

We do this in order that both dependent and independent dimensionless variables be of numerical order one, written $O(1)$. *If* we can do this, then we might suppose *a priori* that derivatives such as $\boldsymbol{\nabla}^* T^*$ ($\boldsymbol{\nabla} = l^{-1}\boldsymbol{\nabla}^*$) will also be of numerical $O(1)$, and the size of various terms will be reflected in certain dimensionless parameters which occur.

In writing (1.10), it is clear that l is a suitable length scale, as it is the size of D. For example, if D was a sphere we might take l as its radius or diameter. We also suppose that the origin is in D; if not, we could write $\mathbf{x} = \mathbf{x}_0 + l\mathbf{x}^*$, where $\mathbf{x}_0 \in D$: evidently $\mathbf{x}^* = O(1)$ in D.

A similar motivation underlies the choice of an 'origin shift' for T. In the absence of a heat source, the temperature will tend to the uniform state $T \equiv T_B$ as $t \to \infty$. If $H \neq 0$, the final state will be raised above T_B (if $H > 0$) by an amount dependent on H. We take ΔT to represent this amount, but we do not know what it is in advance — we will choose it by *scaling*. The subtraction of T_B from T before non-dimensionalisation is because the model for T contains only derivatives of T, so that it is really the variation of T about T_B which we wish to scale.

In a similar way, the time scale t_c is not prescribed in advance, and we will choose it also by scaling, in due course.

With the substitutions in (1.10), the heat equation (1.6) can be written in the form

$$\left(\frac{l^2}{\kappa t_c}\right)\frac{\partial T^*}{\partial t^*} + \left(\frac{Ul}{\kappa}\right)\mathbf{u}^*.\boldsymbol{\nabla}^* T^* = \nabla^{*2} T^* + \left(\frac{Hl^2}{\kappa \Delta T}\right). \tag{1.11}$$

This equation is dimensionless, and the bracketed parameters are dimensionless. They are somewhat arbitrary, since t_c and ΔT have not yet been chosen: we now do so by scaling.

The solution of the equation can depend only on the dimensionless parameters. It is thus convenient to *choose* t_c and ΔT so that two of these are set to some convenient value. There is no unique way to do this.

The temperature scale ΔT appears only in the source term. Since it is this which determines the temperature rise, it is natural to *choose*

$$\Delta T = \frac{Hl^2}{\kappa}. \tag{1.12}$$

It is also customary to choose the time scale so that the two terms of the advective derivative on the left of (1.11) are the same size, and this gives the convective time scale

$$t_c = \frac{l}{U}. \tag{1.13}$$

It is finally also customary (if sometimes confusing) to remove the asterisks (or whatever equivalent symbol is used). If this is done, the dimensionless equation takes the form

$$Pe\left[\frac{\partial T}{\partial t} + \mathbf{u}.\boldsymbol{\nabla} T\right] = \nabla^2 T + 1, \tag{1.14}$$

where the Péclet number is

$$Pe = \frac{Ul}{\kappa}, \tag{1.15}$$

and the solution of the model depends only on this parameter (as well as the initial condition). The boundary condition is

$$T = 0 \ \text{ on } \ \partial D, \tag{1.16}$$

and the initial condition is

$$T = \theta(\mathbf{x}) \ \text{ at } \ t = 0, \tag{1.17}$$

where

$$\theta(\mathbf{x}) = \frac{T_0(l\mathbf{x}) - T_B}{\Delta T}. \tag{1.18}$$

1.2.1 Scaling

A well-scaled problem generally refers to a model in which the dimensionless parameters are $O(1)$ or less. Evidently, this can be ensured simply by dividing through by the largest parameter in any equation. More importantly, if parameters are numerically small, then (as we discuss below) approximate solutions can be obtained by neglecting them. The problem is well-scaled if the resulting approximation makes sense. For example, (1.14) is well-scaled for any value of Pe. However, the problem $\varepsilon T_t = \varepsilon \nabla^2 T + 1$, with $\varepsilon \ll 1$, is not well scaled. One makes a problem well-scaled in this situation by *rescaling* the variables, and we will see examples in our subsequent discussion.

1.2.2 Approximations

Let us consider (1.14) with (1.16) and (1.17), and suppose that $\theta \leq O(1)$. If $Pe \ll 1$, we obtain an approximation by putting $Pe = 0$: $\nabla^2 T + 1 \approx 0$. Evidently, we cannot satisfy the initial condition, and this suggests that we rescale t: put $t = Pe\,\tau$, so that (approximately)

$$\frac{\partial T}{\partial \tau} = \nabla^2 T + 1; \tag{1.19}$$

now we can satisfy the initial condition (at $\tau = 0$) too. Often one abbreviates the rescaling by simply saying, 'rescale $t \sim Pe$, so that $T_t \approx \nabla^2 T + 1$'.

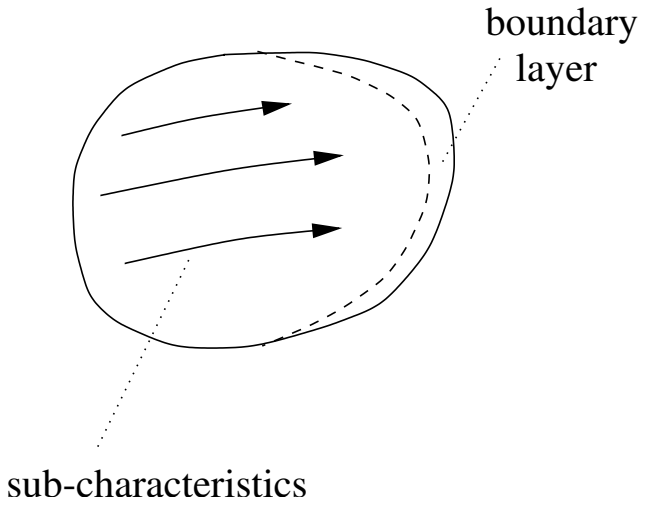

Figure 1.1: Sub-characteristics and boundary layer for the equation (1.14) when $Pe \gg 1$. The sub-characteristics are the flow lines $d\mathbf{x}/dt = \mathbf{u}$, and the boundary layer (of thickness $O(1/Pe)$) is on the part of the boundary where the flow lines terminate.

On the other hand, if $Pe \gg 1$, then $T_t + \mathbf{u}.\boldsymbol{\nabla} T \approx 0$, and we can satisfy the initial condition; but we cannot satisfy the boundary condition on the whole of the boundary ∂D, since the approximating equation is hyperbolic (its characteristics are called 'sub-characteristics'). To remedy this, one has to rescale $\mathbf{x}$ near the part of the

boundary where the boundary condition can not be satisfied, and this is where the sub-characteristics terminate. This gives a spatially thin region, called (evidently) a boundary layer, of thickness $1/Pe$ (see figure 1.1).

Another case to consider is if $\theta \gg 1$, say $\theta \sim \Lambda \gg 1$. We discuss only the case $Pe \gg 1$ (see also question 1.1). Since $T \sim \Lambda$ initially, we need to rescale T, say $T = \Lambda\tilde{T}$. Then $Pe\,[\tilde{T}_t + \mathbf{u}.\boldsymbol{\nabla}\tilde{T}] = \nabla^2\tilde{T} + \dfrac{1}{\Lambda}$, and with $\tilde{T} = O(1)$, we have $\tilde{T}_t + \mathbf{u}.\boldsymbol{\nabla}\tilde{T} \approx 0$ for $Pe \gg 1$. The initial function is simply advected along the flow lines (sub-characteristics), and the boundary condition $\tilde{T} = 0$ is advected across D. In a time of $O(1)$, the initial condition is 'washed out' of the domain. Following this, we revert to T, thus $T_t + \mathbf{u}.\boldsymbol{\nabla}T = \dfrac{1}{Pe}(\nabla^2 T + 1)$. Evidently T will remain ≈ 0 in most of D, and in fact $T \sim O\left(\dfrac{1}{Pe}\right)$. Putting $T = \dfrac{\chi}{Pe}$, χ satisifies $\chi_t + \mathbf{u}.\boldsymbol{\nabla}\chi = \dfrac{1}{Pe}\nabla^2\chi + 1$, and there is a boundary layer near the boundary as shown in figure 1.1. If n is the coordinate normal to ∂D in this layer, then $n \sim \dfrac{1}{Pe}$ in the boundary layer. The final steady state has $T \sim \dfrac{1}{Pe}$, and this applies also for $\theta \lesssim O(1)$.

These ideas of perturbation methods are very powerful, but a full exposition is beyond the scope of this book. Nevertheless, they will relentlessly inform our discussion. While it is possible to use formal perturbation expansions, it is sufficient in many cases to give more heuristic forms of argument, and this will typically be the style we choose.

1.3 Qualitative methods for differential equations

The language of the description of continuous processes is the language of differential equations, and these will form the instrument of our discussion. The simplest differential equation is the ordinary differential equation, and the simplest ordinary differential equation (or ODE) is the first order autonomous equation

$$\dot{x} = f(x), \tag{1.20}$$

where the notation $\dot{x} \equiv \dfrac{dx}{dt}$ indicates the first derivative, and the use of an overdot is normally associated with the use of time t as the independent variable, i.e., $\dot{x} = dx/dt$.

The solution of (1.20) with initial condition $x(t_0) = x_0$ can be written as the *quadrature*

$$t = t_0 + \int_{x_0}^{x} \frac{d\xi}{f(\xi)}, \tag{1.21}$$

and, depending on the function f, this may be inverted to find x explicitly. So, for example, the solution of $\dot{x} = 1 - x^2$ is $x = \tanh(t + c)$ (if $|x(t_0)| < 1$).

Going on with this latter example, we see that $x \to 1$ as $t \to \infty$ (and $x \to -1$ as $t \to -\infty$), and in practice, this may be all we want to know. If a population is subject to constant immigration and removal by mutual pair destruction, so that

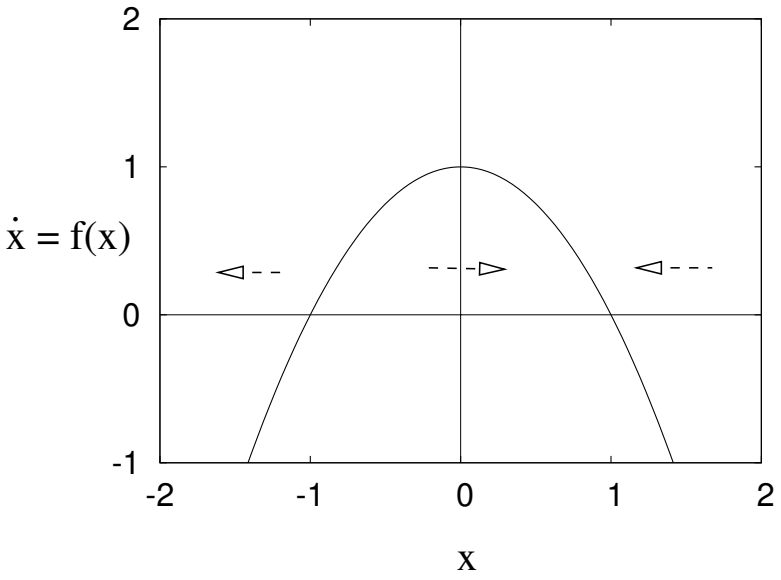

Figure 1.2: The evolution of the solutions of $\dot{x} = f(x)$ (here $f = 1 - x^2$) depends only on the sign of x.

$\dot{x} = 1 - x^2$, then after a transient (a period of time dependence), the population will equilibrate stably to $x = 1$. But to ascertain this, all we need to know is the shape of the curve $f(x) = 1 - x^2$. Simply by finding the zeros of $1 - x^2$ and the slope of the graph there, we can immediately infer that for all initial values $x(0) > -1$, $x \to 1$ as $t \to \infty$, while if $x(0) < -1$, then $x \to -\infty$ as $t \to -\infty$: see figure 1.2. And this can be done for *any* function $f(x)$ in the equation $\dot{x} = f(x)$.

This simple example carries an important message. Approximate or qualitative methods may be just as useful, or more useful, than the ability to obtain exact results. An extension of this insight suggests that it may often be the case that approximate analytic insights can provide more information than precise, computational results.

1.3.1 Oscillations

If we move from first order systems to second order systems of the form

$$\begin{aligned} \dot{x} &= f(x, y), \\ \dot{y} &= g(x, y), \end{aligned} \tag{1.22}$$

more interesting phenomena can occur. This is the subject of phase plane analysis, and the fundamental distinction between first and second order systems is that periodic oscillations can occur. An illuminating example is illustrated in figure 1.3, and is typified by (but is not restricted to) the equations

$$\begin{aligned} \dot{x} &= y - g(x), \\ \dot{y} &= h(x) - y, \end{aligned} \tag{1.23}$$

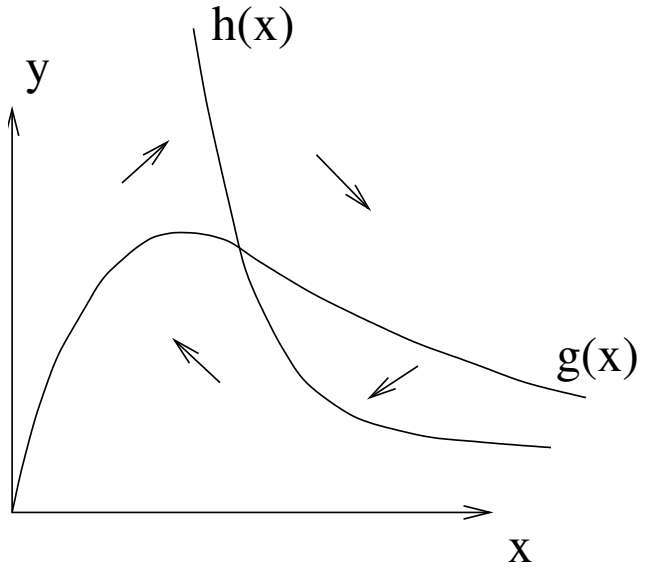

Figure 1.3: Nullclines for (1.23).

where the functions g and h are as shown in the figure: g is unimodal (e. g., like $g = xe^{-x}$) and h is monotonic decreasing (e. g., like $h = 1/(x - c)$). The graphs of $g(x)$ and $h(x)$ (and more generally, the curves where $\dot{x} = 0$ and $\dot{y} = 0$) are called the nullclines of x and y, and it is simple to see that where they intersect, there is a steady state solution, and also that in the four regions separated by the nullclines, the trajectories wind round the fixed point in a clockwise manner.

The next issue is whether the fixed point is unstable. If we denote it as (x^*, y^*), write $x = x^* + X$, $y = y^* + Y$, and linearise for small X and Y, then

$$\dot{\mathbf{U}} \approx \begin{pmatrix} -g' & 1 \\ h' & -1 \end{pmatrix} \mathbf{U}, \tag{1.24}$$

where $\mathbf{U} = \begin{pmatrix} X \\ Y \end{pmatrix}$, and the derivatives are evaluated at the fixed point. The stability of such a two by two system with community matrix $A = \begin{pmatrix} -g' & 1 \\ h' & -1 \end{pmatrix}$ is governed by the trace and determinant of A. Solutions of (1.24) proportional to $e^{\sigma t}$ exist if $\sigma^2 - \sigma \operatorname{tr} A + \det A = 0$, and this delineates the stability regions in the $(\operatorname{tr} A, \det A)$ space as indicated in figure 1.4. In the present case, $\operatorname{tr} A = -g' - 1$, $\det A = g' - h'$, so that for the situation shown in figure 1.3, where $h' < g' < 0$, $\det A > 0$, and the fixed point is an unstable spiral (or node) if $g' < -1$. When $g' = -1$, there is a Hopf bifurcation, and if the system has bounded trajectories (as is normal for a model of a physical process) then one expects a stable periodic solution to exist. Figure 1.5 illustrates a possible example.

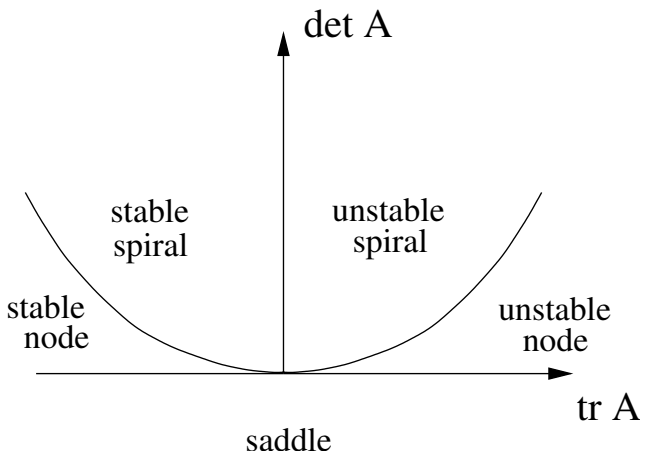

Figure 1.4: Characterisation of fixed point stability in terms of trace and determinant of the community matrix A. The curve separating spirals from nodes is given by $\det A = \frac{1}{4}(\mathrm{tr}\, A)^2$.

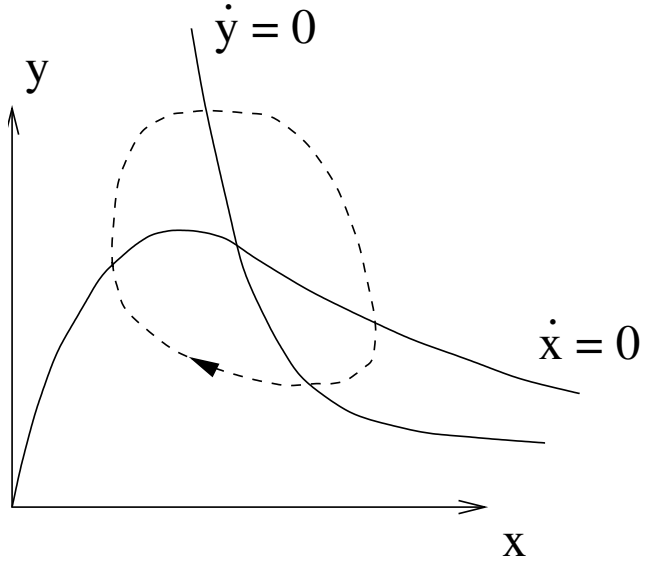

Figure 1.5: Typical form of limit cycle for a system with nullclines as in figure 1.3.

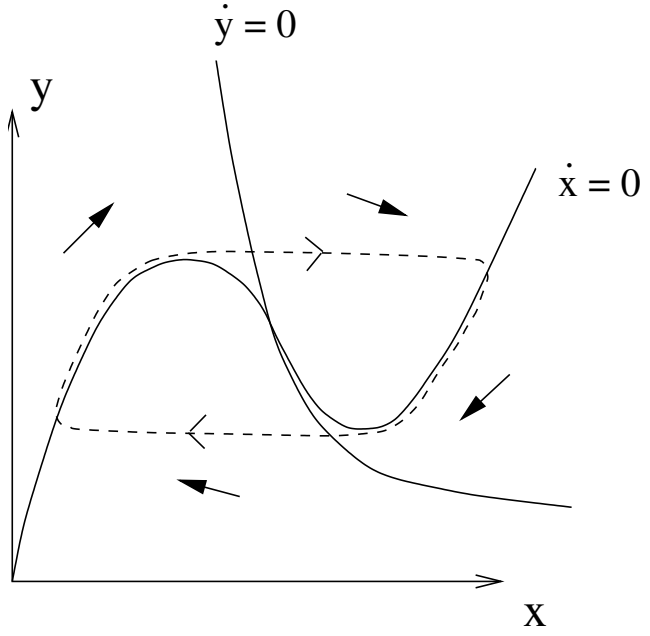

Figure 1.6: Typical form of relaxation oscillation in phase plane for (1.25).

1.3.2 Relaxation oscillations

It is a general precept of the applied mathematician that there are three kinds of numbers: small, large, and of order one. And the chances of a number being $O(1)$ are not great. Thus for systems of the form (1.22), it is often the case in practice that the time scales for each equation are different, so that in suitable dimensionless units, the second order system (1.23) might take the form

$$\begin{aligned} \varepsilon \dot{x} &= y - g(x), \\ \dot{y} &= h(x) - y, \end{aligned} \tag{1.25}$$

where the parameter ε is small. Now suppose that the nullclines $y = g(x)$ and $y = h(x)$ for the system (1.25) are as shown in figure 1.6, i. e., g has a cubic shape. Trajectories rotate clockwise, and linearisation about the fixed point yields a community matrix A with $\operatorname{tr} A = -(g'/\varepsilon) - 1$, $\det A = (g' - h')/\varepsilon$, thus with $g' > h'$, the fixed point is a spiral or node, and with $\varepsilon \ll 1$, $\operatorname{tr} A \approx -g'/\varepsilon > 0$, so it is unstable. Thus we expect a limit cycle, and because $\varepsilon \ll 1$, this takes the form of a *relaxation oscillation* in which the trajectory jumps rapidly backwards and forwards between branches of the x nullcline. For $\varepsilon \ll 1$, x rapidly jumps to its quasi-equilibrium $y \approx g(x)$, and then y migrates slowly ($\dot{x} \approx [h(x) - g(x)]/g'(x)$) until $g' = 0$ and x jumps rapidly to the other branch of g. Figure 1.7 shows the time series of the resulting oscillation. The motion is called 'relaxational' because the fast variable x 'relaxes' rapidly to a quasi-stationary state after each transient excursion.

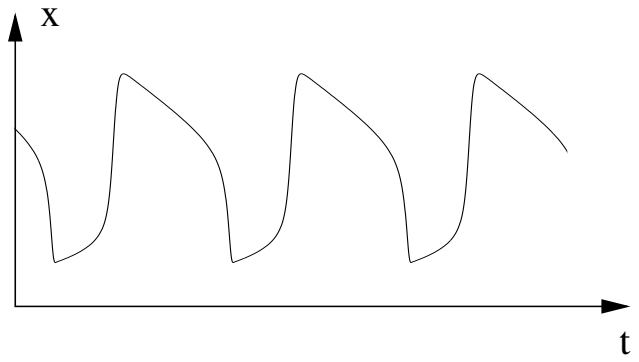

Figure 1.7: Time series for x corresponding to figure 1.6.

1.3.3 Hysteresis

Lighting a match is an everyday experience, but an understanding of why it occurs is less obvious. As the match is lit, a reaction starts to occur which is exothermic, i. e., it releases heat. The amount of heat released is proportional to the rate of reaction, and this itself increases with temperature (coal burns when hot, but not at room temperature). The heat released is given by the Arrhenius expression $A\exp(-E/RT)$, where E is the activation energy, R is the gas constant, T is the absolute temperature, and we take A as constant (it actually depends on reactant concentration). A simple model for the match temperature is then

$$c\frac{dT}{dt} = -k(T - T_0) + A\exp(-E/RT), \tag{1.26}$$

where c is a suitable specific heat capacity, k is a cooling rate coefficient, and T_0 is ambient (e. g., room) temperature. The terms on the right represent the source term due to the reactive heat release, and a Newtonian cooling term (cooling rate proportional to temperature excess over the surroundings).

We can solve (1.26) as a quadrature, but it is much simpler to look at the problem graphically. Bearing in mind that T is absolute temperature, the source and sink terms typically have the form shown in figure 1.8, and we can see that there are three equilibria, and the lowest and highest ones are stable. Of course, one could have only the low equilibrium (for example, if k is large or T_0 is low) or the high equilibrium (if k is small or T_0 is high). The low equilibrium corresponds to the quiescent state — the match in the matchbox; the high one is the match alight. If we vary T_0, then the equilibrium excess temperature Δ $(= T - T_0)$ varies as shown in figure 1.9: the upper and lower branches are stable.

We can model lighting a match as a local perturbation to Δ; the heat of friction in striking a match raises the temperature excess from near zero to a value above the unstable equilibrium on the middle branch, and Δ then migrates to the stable upper

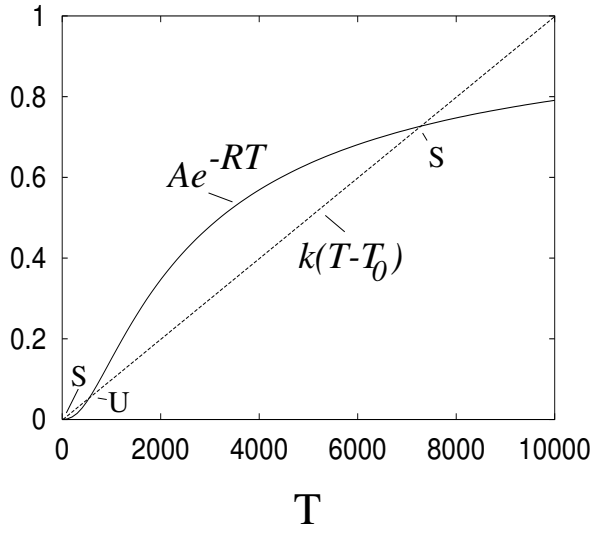

Figure 1.8: Plots of the functions $A\exp[-E/R(T+T_m)]$ and $k(T-T_0)$ using values $T_m = 273$ (so T is measured in centigrade), with values $A = 1$, $E = 20,000$, $R = 8.3$, $k = 10^{-4}$, $T_0 = 15^\circ$ C.

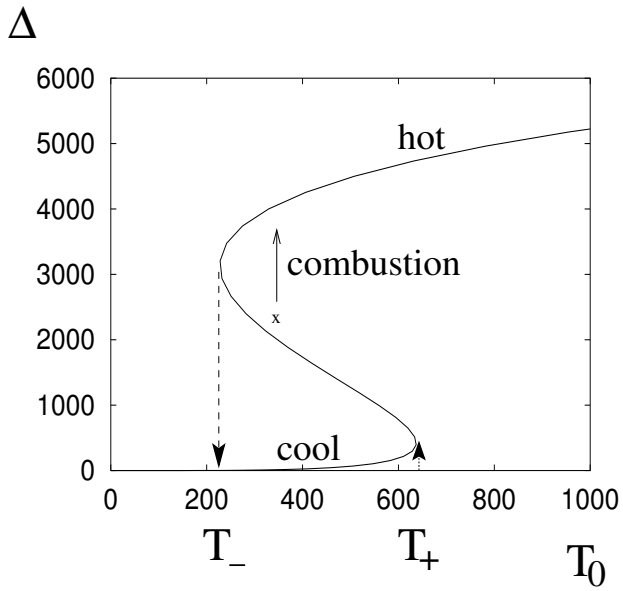

Figure 1.9: Equlibrium curve for Δ_0 as a function of T_0, parameters as for figure 1.8, but $E = 35,000$. An initial condition above the unstable middle branch leads to combustion.

branch, where the reaction (like that of a coal fire) is self-perpetuating. Figure 1.9 also explains why it is difficult to light a wet match, but a match will spontaneously light if held at some distance above a lighted candle.

Figure 1.9 exhibits a form of hysteresis, meaning non-reversibility. Suppose we place a (very large, so it will not burn out) match in an oven, and we slowly raise the ambient temperature from a very low value to a very high value, and then lower it once again. Because the variation is slow, the excess temperature will follow the equilibrium curve in figure 1.9. At the value T_+, Δ suddenly jumps (spontaneous combustion) to the hot branch, and remains on this if T_0 is increased further. Now if T_0 is decreased, Δ remains on the hot branch until $T_0 = T_-$, below which it suddenly drops to the cool branch again (extinction).[1] The path traced out in the $(T_0, \Delta T)$ plane is not reversible (it is not an arc but a closed curve).

The reason the multiple equilibria exist (at least for matches) is that for many reactions, E/R is very large and also A is very large. This just says that it is possible that $Ae^{-E/RT}$ is very small near T_0 but jumps rapidly at higher T to a large asymptote. To be more specific, we non-dimensionalise (1.26) by putting

$$T = T_0 + (\Delta T)\theta, \quad t = [t]t^*, \tag{1.27}$$

and in fact we choose the cooling time scale $[t] = c/k$. Then we have, dropping the asterisk, and after some simplification,

$$\dot{\theta} = -\theta + \frac{A}{k\Delta T} \exp\left(-\frac{E}{RT_0}\right) \exp\left[\frac{E\Delta T}{RT_0^2} \frac{\theta}{1+\varepsilon\theta}\right], \tag{1.28}$$

where $\varepsilon = \Delta T/T_0$. The temperature rise scale ΔT has to be chosen, and there are two natural choices: to set the exponent coefficient $E\Delta T/RT_0^2$ to one, or the pre-multiplicative constant to one. In one way, the latter seems the better choice: it seems to balance the source with the sink. But because E/R is large, we might then find $E\Delta T/RT_0^2$ to be large, which would ruin the intention. So we choose (but it does not really matter)

$$\Delta T = \frac{RT_0^2}{E}, \tag{1.29}$$

so that

$$\dot{\theta} = -\theta + \lambda \exp\left[\frac{\theta}{1+\varepsilon\theta}\right], \tag{1.30}$$

where

$$\lambda = \frac{EA}{kRT_0^2} \exp\left(-\frac{E}{RT_0}\right), \quad \varepsilon = \frac{RT_0}{E}. \tag{1.31}$$

If typical values are $T_0 = 300$ K, $E/R = 10,000$ K, we see that $\varepsilon \ll 1$, and also, since

$$\lambda = \frac{\lambda_0}{\varepsilon^2} \exp\left(-\frac{1}{\varepsilon}\right), \quad \lambda_0 = \frac{AR}{kE}, \tag{1.32}$$

[1] We can understand why T follows the equilibrium curve as follows. We can write (1.26) in terms of suitable dimensionless variables as $\dot{\Delta} = T_0 - g(\Delta)$, where $g(\Delta)$ is a cubic-like curve similar to the function $T_0(\Delta)$ depicted in figure 1.9. if T_0 is slowly varying, then $T_0 = T_0(\delta t)$ where $\delta \ll 1$, and putting $\tau = \delta t$, we have $\delta d\Delta/d\tau = T_0(\tau) - g(\Delta)$; thus on the slow time scale τ, Δ will tend rapidly to a (quasi-equilibrium) zero of the right hand side.

λ is extremely sensitive to ε and thus T_0.

So long as $\theta = O(1)$, or at least $\theta \ll 1/\varepsilon$ (i.e. $T - T_0 \ll T_0$), we can neglect the $\varepsilon\theta$ term, so that

$$\dot{\theta} \approx -\theta + \lambda e^{\theta}. \tag{1.33}$$

This gives the lower part of the S-shaped curve in figure 1.9, and the equilibria are given by $\theta e^{-\theta} = \lambda$, the roots of which coalesce and disappear if $\lambda > e^{-1}$. This corresponds to the value of $T_0 = T_+$ in figure 1.9, and implies

$$\frac{E}{RT_+} \approx 1 + \ln\lambda_0 + 2\ln\left(\frac{E}{RT_+}\right). \tag{1.34}$$

There are two roots to this, but only one has $E/RT_+ \gg 1$. Further, since $x \gg 2\ln x$ if $x \gg 1$, we have, approximately,

$$T_+ \approx \frac{E}{R[1 + \ln\lambda_0 + 2\ln\{1 + \ln\lambda_0\}]}. \tag{1.35}$$

If $E/R \gg T_0$, then the fact that one can light matches at room temperature suggests that λ_0 is large, and specifically $\ln\lambda_0 \sim E/RT_0$. (Note that this does not imply $\lambda = O(1)$.)

Carrying on in this vein, let us suppose that we define a temperature T_c by

$$\lambda_0 = \exp\left[\frac{E}{RT_c}\right], \tag{1.36}$$

and we suppose $T_c \sim T_0$. It follows that $T_+ \approx T_c$, or more precisely,

$$T_+ \approx \frac{T_c}{1 + \varepsilon_c\{1 + 2\ln(1 + \varepsilon_c^{-1})\}}, \tag{1.37}$$

where $\varepsilon_c = RT_c/E$. The stable cool branch and unstable middle branch are then the roots of

$$\theta e^{-\theta} \approx \lambda = \frac{1}{\varepsilon^2}\exp\left[-\frac{1}{\varepsilon}\left(1 - \frac{T_0}{T_c}\right)\right], \tag{1.38}$$

and in general $\lambda \ll 1$ (if $T_0 < T_c$), so that we find the stable cool branch (when $\theta \ll 1$)

$$\theta \approx \lambda \approx \left(\frac{E}{RT_0}\right)^2 \exp\left[\frac{E}{R}\left(\frac{1}{T_c} - \frac{1}{T_0}\right)\right], \tag{1.39}$$

and the unstable middle branch (where $\theta \gg 1$),

$$\theta \approx \frac{1}{\varepsilon}\left(1 - \frac{T_0}{T_c}\right) + O(|\ln\varepsilon|) \approx \frac{E}{R}\left(\frac{1}{T_0} - \frac{1}{T_c}\right). \tag{1.40}$$

Evidently θ becomes $O(1/\varepsilon)$ on the middle branch, and to allow for this, we put

$$\theta = \Theta/\varepsilon, \tag{1.41}$$

and (1.30) becomes

$$\dot{\Theta} = -\Theta + \frac{1}{\varepsilon}\exp\left[\frac{1}{\varepsilon}\left\{\frac{\Theta}{1+\Theta} - \left(1 - \frac{T_0}{T_c}\right)\right\}\right]. \tag{1.42}$$

Equating the right hand side to zero gives an equilibrium which can be written approximately as [2]

$$\Theta \approx \frac{T_c - T_0}{T_0} + O(\varepsilon|\ln\varepsilon|), \tag{1.43}$$

and Θ tends to infinity as $T_0 \to 0$. The hot branch is recovered for even higher values of Θ, so that $\Theta \gg 1$, in which case the equilibrium of (1.42) is given by

$$\Theta \approx \frac{1}{\varepsilon}\exp\left[\frac{T_0}{\varepsilon T_c}\right], \tag{1.44}$$

and increases again with T_0.

At a fixed value of T_0 (and thus λ), the critical value of T for ignition is that on the unstable middle branch, as this gives the necessary temperature which must be generated in order for combustion to occur. From (1.43) (ignoring terms in ε), this can be written dimensionally in the simple approximate form

$$T \approx T_c, \tag{1.45}$$

which is approximately the critical temperature at the nose of the curve in figure 1.9. The fact that T is approximately constant on the unstable branch is due to the steepness of the exponential curve in figure 1.8, which is in turn due to the large value of E/R. In terms of the parameters of the problem, the critical (ignition) temperature is thus

$$T_c \approx \frac{E}{R\ln\left(\dfrac{AR}{kE}\right)}. \tag{1.46}$$

Hysteresis and multiplicity of solutions is a theme which will recur again and again in this book.

1.3.4 Resonance

Swinging a pendulum is an everyday experience, and one which students learn about in a first year mechanics course. If the point of suspension itself oscillates, then one has a forced pendulum, and an interesting phenomenon occurs. At low forcing frequencies, the pendulum oscillates in phase with the oscillating point of support. At high forcing frequencies, it oscillates out of phase with the support. Moreover, this change in phase appears to occur abruptly, at a particular value of the forcing frequency. At the same time, there is also a sudden rise in amplitude of the motion, although it is less easy to see this in a casual experiment. This observation is associated with the phenomenon of resonance, and can be easily experienced by jumping on a springboard.

[2] Note that as $T_0 \to T_c$, (1.43) matches with (1.40).

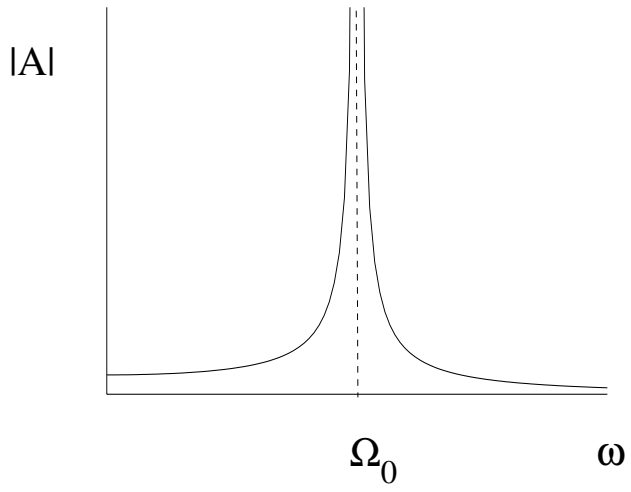

Figure 1.10: Resonant amplitude response.

To illustrate the phenomenon of resonance mathematically, we solve the equation of a forced oscillator, and an example of such a system is the forced pendulum. To be specific, we take as a model equation

$$\ddot{u} + \beta\dot{u} + \Omega_0^2 \sin u = \varepsilon \sin \omega t. \tag{1.47}$$

This represents the motion of a damped, non-linear pendulum, with a forcing on the right hand side which mimics (it is not a precise model) the effect on the pendulum of an oscillating support. We suppose that the model is dimensionless, and that ε is small, so that the response amplitude of u will be also. We also suppose that the damping term β is small.

The simplest approximation of (1.47) neglects β altogether, and linearises $\sin u$, so that

$$\ddot{u} + \Omega_0^2 u \approx \varepsilon \sin \omega t, \tag{1.48}$$

to which the forced solution is

$$u = A \sin \omega t, \tag{1.49}$$

where the response amplitude A is given by

$$A = \frac{\varepsilon}{\Omega_0^2 - \omega^2}. \tag{1.50}$$

Plotting $|A|$ versus ω gives the familiar resonant response diagram of figure 1.10, in which the amplitude tends to infinity as $\omega \to \Omega_0$. (If one actually solves (1.48) at $\omega = \Omega_0$, one obtains a solution whose amplitude grows linearly in time.)

The two effects we have neglected, damping and non-linearity, have two separate effects on this diagram. If we include only damping, so that

$$\ddot{u} + \beta\dot{u} + \Omega_0^2 u = \varepsilon \operatorname{Im} e^{i\omega t}, \tag{1.51}$$

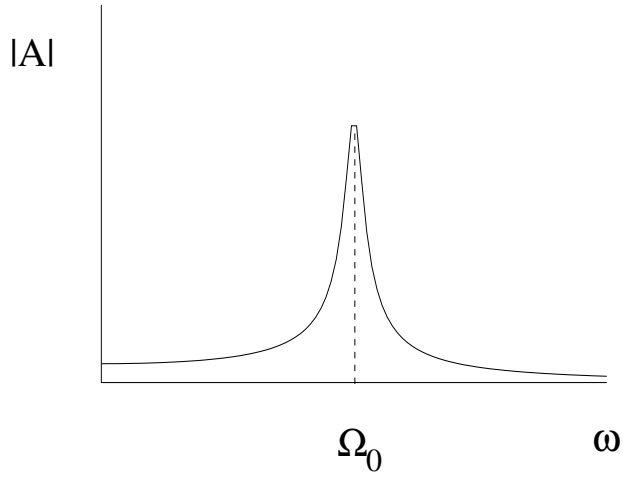

Figure 1.11: Resonant amplitude response with damping.

then the forced solution is again

$$u = \mathrm{Im}\,[Ae^{i\omega t}], \tag{1.52}$$

where now

$$A = \frac{\varepsilon}{\Omega_0^2 + i\beta\omega - \omega^2}, \tag{1.53}$$

and the presence of the damping term causes a phase shift which caps the response amplitude, as shown in figure 1.11, since

$$|A| = \frac{\varepsilon}{[(\Omega_0^2 - \omega^2)^2 + \beta^2\omega^2]^{1/2}}; \tag{1.54}$$

the peak amplitude at resonance is $|A| = \varepsilon/\beta\omega$.

The other effect is nonlinearity, which is less easy to deal with. In fact, one can use perturbation methods to assess its effect in a formal manner, but our present purpose is more rough and ready. Our idea is this: resonance occurs when the forcing frequency ω equals the frequency of the underlying oscillator. The difference which occurs for a nonlinear pendulum is that this frequency (call it Ω) now depends on the amplitude of the oscillation A: $\Omega = \Omega(A)$.

To be specific, we again put $\beta = 0$, and consider simply the unforced pendulum:

$$\ddot{u} + \Omega_0^2 \sin u = 0. \tag{1.55}$$

A first (energy) integral is

$$\tfrac{1}{2}\dot{u}^2 + \Omega_0^2(1 - \cos u) = E, \tag{1.56}$$

where E is constant (and depends on amplitude, with $E(A)$ increasing with A). The phase plane is shown in figure 1.12 and is symmetric about both u and $\dot{u}$ axes. Thus

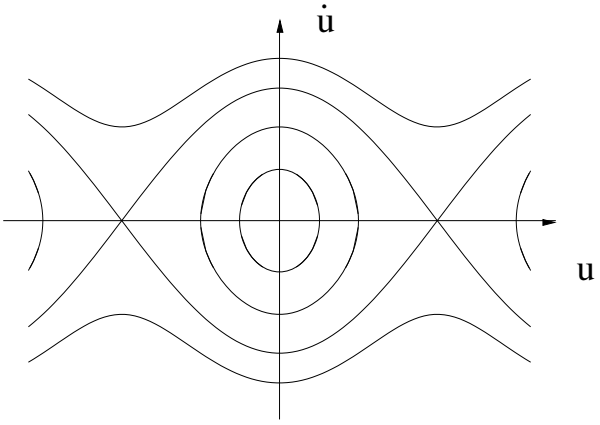

Figure 1.12: Phase plane for the simple pendulum.

a quadrature of (1.56) implies the period P is given by

$$P = \frac{2\sqrt{2}}{\Omega_0} \int_0^A \frac{du}{[\cos u - \cos A]^{1/2}}, \tag{1.57}$$

where we have used the fact that the amplitude A is given by

$$E = \Omega_0^2 (1 - \cos A). \tag{1.58}$$

From (1.57), we find that the frequency $\Omega = 2\pi/P$ is given by

$$\Omega(A) = \frac{\pi \Omega_0}{\sqrt{2} \displaystyle\int_0^A \frac{du}{[\cos u - \cos A]^{1/2}}}. \tag{1.59}$$

Ω is a monotonically decreasing function of A in $(0, \pi)$, with $\Omega(0) = \Omega_0$ and $\Omega(\pi) = 0$, and this is represented as the dotted curve in figure 1.13.

Without now actually solving the forced, damped, nonlinear equation, we can guess intelligently what happens. For small amplitude oscillations, $|A|$ starts to increase as ω approaches Ω_0; but as $|A|$ increases, the natural frequency Ω decreases, and as it is the approach of ω to the natural frequency which is the instrument of resonance, so the amplitude response curve bends round, as shown in figure 1.13, to try and approach the dotted $\Omega(A)$ curve. Finally, the effect of damping can be expected to be as in the linear case, to put a cap on the two asymptotes to $\Omega(A)$. Thus, we infer the response diagram shown in figure 1.13, and this is in fact correct. Moreover, (1.50) suggests $A \gtrless 0$ for $\omega \lessgtr \Omega_0$, i. e., the solution is in phase with the forcing for $\omega < \Omega_0$, and out of phase for $\omega > \Omega_0$. Extending this to the nonlinear case, we infer that at low frequencies, the response is in phase, but that it is out of phase at high frequencies (as observed).

The response also involves hysteresis (if damping is small enough). If ω is increased gradually, then at a value $\omega_+ < \Omega_0$, there is a sudden jump to an out of phase

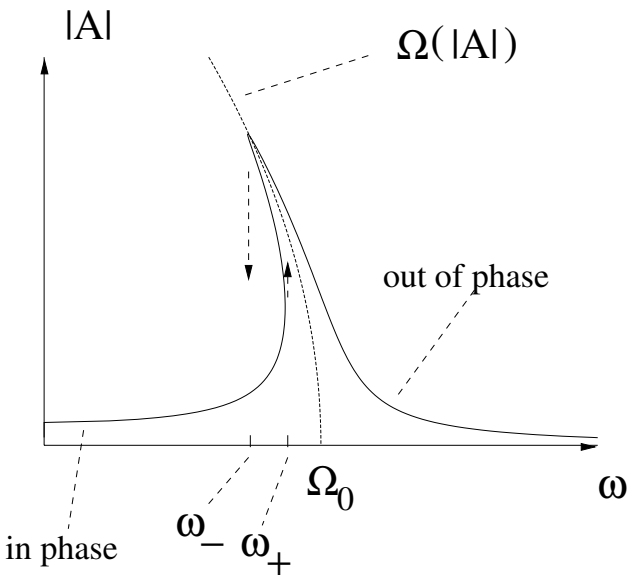

Figure 1.13: Nonlinearity bends the resonant response curve, producing hysteresis.

oscillation with higher amplitude. Equivalently, as ω is reduced for this high frequency response there is a sudden jump down in amplitude to an in-phase oscillation at a value $\omega_- < \omega_+$. This response diagram explains what one sees in the simple experiment and illustrates the important effects of nonlinearity.

1.4 Qualitative methods for partial differential equations

Any introductory course on partial differential equations will provide the classification of second order partial differential equations into the three categories: elliptic, parabolic, hyperbolic; and one also finds the three simple representatives of these: Laplace's equation $\nabla^2 u = 0$, governing steady state temperature distribution (for example); the heat equation $u_t = \nabla^2 u$, which describes diffusion of heat (or solute); and the wave equation $u_{tt} = \nabla^2 u$, which describes the oscillations of a string or of a drum. These equations are of fundamental importance, as they describe diffusion or wave propagation in many other physical processes, but they are also linear equations; however the way in which they behave carries across to nonlinear equations, but of course nonlinear equations have other behaviours as well.

1.4.1 Waves

In the linear wave equation (in one dimension, describing waves on strings) $u_{tt} = c^2 u_{xx}$, the general solution is $u = f(x+ct)+g(x-ct)$, and represents the superposition of two travelling waves of speed c moving in opposite directions. In more than one space dimension, the equivalent model is $u_{tt} = c^2\nabla^2 u$, and the solutions are functions

of $(\mathbf{k}.\mathbf{x} \pm \omega t)$, where ω is frequency and $\mathbf{k}$ is the wave vector; the waves move in the direction of the vector $\mathbf{k}$, while the wave speed is then $c = \omega/|\mathbf{k}|$.

Even simpler to discuss is the first order wave equation

$$u_t + cu_x = 0, \tag{1.60}$$

which is trivially solved by the method of characteristics to give

$$u = f(x - ct), \tag{1.61}$$

representing a wave of speed c. The idea of finding characteristics generalises to systems of the form

$$A\mathbf{u}_t + B\mathbf{u}_x = \mathbf{0}, \tag{1.62}$$

where $\mathbf{u} \in \mathbf{R}^n$ and A and B are constant $n \times n$ matrices. We can solve this system as follows. The eigenvalue problem

$$\lambda A\mathbf{w} = B\mathbf{w} \tag{1.63}$$

will in general have n solution pairs $(\mathbf{w}, \lambda)$, where each value of λ is one of the roots of the n-th order polynomial

$$\det(\lambda A - B) = 0. \tag{1.64}$$

Suppose the n eigenvalues λ_i, $i = 1, \ldots, n$, are distinct (which is the general case); then the corresponding $\mathbf{w}_i$ are independent, and the matrix P formed by the eigenvectors as columns (i.e., $P = (\mathbf{w}_1, ..., \mathbf{w}_n)$) satisfies $BP = APD$, where D is the diagonal matrix $\mathrm{diag}(\lambda_1, ..., \lambda_n)$. P is invertible, and if we write $\mathbf{v} = P^{-1}\mathbf{u}$, then $AP\mathbf{v}_t + BP\mathbf{v}_x = 0$, whence $\mathbf{v}_t + D\mathbf{v}_x = 0$, and the general solution is

$$\mathbf{u} = P\mathbf{v} = \sum_{i,j} P_{ij} f_j(x - \lambda_j t)\mathbf{e}_i, \tag{1.65}$$

where $\mathbf{e}_i$ is the i-th unit vector, and the functions f_j are arbitrary; this represents the superposition of n travelling waves with speeds λ_i. This procedure works providing A is invertible, and also (practically) if all the λ_i are real, in which case we say the system is hyperbolic.

More generally, we can use the above prescription to solve the nonlinear equation

$$A\mathbf{u}_t + B\mathbf{u}_x = \mathbf{r}(x, t, \mathbf{u}), \tag{1.66}$$

where we allow A and B to depend on x and t also. The diagonalisation procedure works exactly as before, leading to

$$A\frac{\partial}{\partial t}(P\mathbf{v}) + B\frac{\partial}{\partial x}(P\mathbf{v}) = \mathbf{r}[x, t, P\mathbf{v}]; \tag{1.67}$$

now, however, λ, $\mathbf{w}$ and therefore also P will depend on x and t. Thus we find

$$\mathbf{v}_t + D\mathbf{v}_x = P^{-1}A^{-1}\mathbf{r} - [P^{-1}P_t + DP^{-1}P_x]\mathbf{v}, \tag{1.68}$$

and the components of $\mathbf{v}$ can be solved as a set of coupled ordinary differential equations along the characteristics $dx/dt = \lambda_i$.

If A and B depend also on $\mathbf{u}$ (the *quasi-linear* case), the procedure is less simple for systems. The characterisation of the system as hyperbolic based on the reality of the eigenvalues of (1.63) is still appropriate, but the diagonalisation and reduction to the equivalent of (1.68) are less clear. In the particular case where P depends only on $\mathbf{u}$ (and not on x and t), and if P^{-1} is a Jacobian matrix (i. e., $(P^{-1})_{ij} = \dfrac{\partial v_i}{\partial u_j}$ for some vector $\mathbf{v}(\mathbf{u})$), then the function $\mathbf{v}$ is given by the (well-defined) line integral

$$\mathbf{v} = \int P^{-1}\, d\mathbf{u}, \tag{1.69}$$

and $\mathbf{v}_t = P^{-1}\mathbf{u}_t$, $\mathbf{v}_x = P^{-1}\mathbf{u}_x$; hence we can derive the diagonalised form

$$\mathbf{v}_t + D\mathbf{v}_x = P^{-1}A^{-1}\mathbf{r}. \tag{1.70}$$

This shows how the characteristic equations can be derived, but in general the equations can not be solved, since the elements of D will depend on all the components of $\mathbf{v}$. An example of this type occurs in river flow, and will be discussed in chapter 4.

However, the method of characteristics always works in one dimension, so we now return our attention to this case. Consider as an example the nonlinear evolution equation

$$u_t + uu_x = 0, \tag{1.71}$$

to be solved on the whole real axis. The method of characteristics leads to the implicitly defined general solution

$$u = f(x - ut), \tag{1.72}$$

which is analogous to (1.61), and represents a wave whose *speed depends on its amplitude*. Thus higher values of u propagate more rapidly, and this leads to the wave steepening depicted in figure 1.14.

In fact, it can be seen that eventually u becomes multi-valued, and this signifies a break down of the solution. The usual way in which this multi-valuedness is avoided is to allow the formation of a *shock*, which consists of a point of discontinuity of u. The characteristic solution applies in front of and behind the shock, and the characteristics intersect at the shock, whose propagation forwards is described by an appropriate *jump condition*: see figure 1.15.

This seemingly arbitrary escape route is motivated by the fact that evolution equations such as (1.71) are generally derived from a conservation law, here of the form

$$\frac{d}{dt}\int_A^B u\, dx = -[\tfrac{1}{2}u^2]_A^B, \tag{1.73}$$

where the square-bracketed term represents the jump in $\frac{1}{2}u^2$ between A and B. The deduction of the point form (1.71) from (1.73) required the additional assumption that u was continuously differentiable; however, it is possible to satisfy (1.73) at a

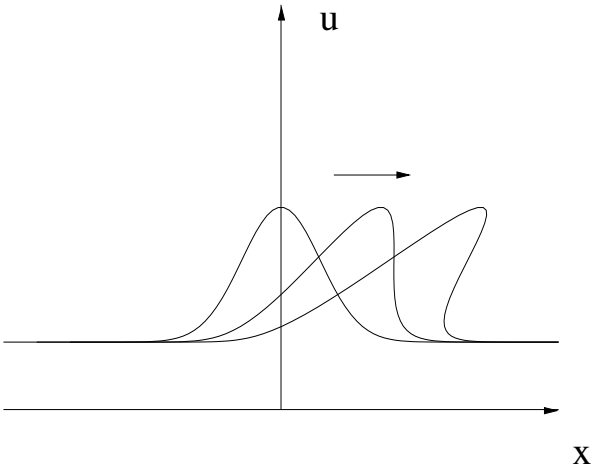

Figure 1.14: Nonlinearity causes wave steepening.

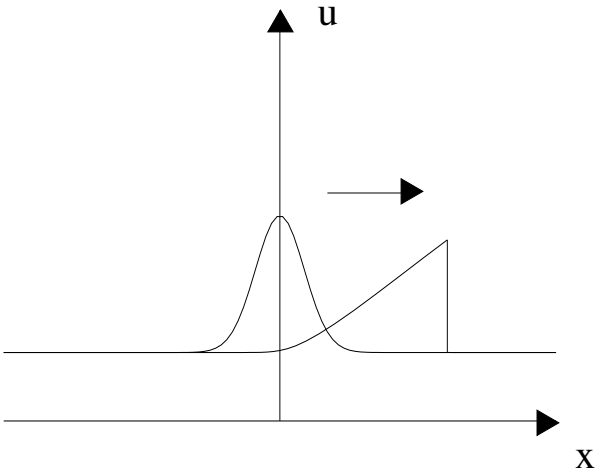

Figure 1.15: Intersection of characteristics leads to shock formation.

point of discontinuity of u. Suppose u is discontinuous at $x = x_S(t)$, and denote the jump in a quantity q across the shock by $[q]^+_- = q(x_{S^+}, t) - q(x_{S^-}, t)$. Then by letting $B \to x_{S^+}$, $A \to x_{S^-}$, we find that (1.73) implies the jump condition

$$\dot{x}_S = \frac{[\frac{1}{2}u^2]^+_-}{[u]^+_-} = \tfrac{1}{2}(u_+ + u_-). \tag{1.74}$$

An example

We illustrate how to solve a problem of this type by considering the initial function for u

$$u = u_0(x) = \frac{1}{1+x^2} \quad \text{at} \quad t = 0. \tag{1.75}$$

The implicitly defined solution is then

$$u = \frac{1}{1+(x-ut)^2}, \tag{1.76}$$

or, in characteristic form,

$$u = u_0(\xi) = \frac{1}{1+\xi^2}, \quad x = \xi + ut. \tag{1.77}$$

This defines a single-valued function so long as u_x is finite everywhere. Differentiating (1.77) leads to

$$u_x = \frac{u_0'(\xi)}{1+tu_0'(\xi)}, \tag{1.78}$$

and this shows that $u_x \to -\infty$ as $t \to t_c = \min\limits_{\xi\,:\,u_0'<0}\left[-\dfrac{1}{u_0'(\xi)}\right]$. Since $-u_0' = 2\xi/(1+\xi^2)^2$, we find the relevant value of ξ is $1/\sqrt{3}$, and thus $t_c = \dfrac{8}{3\sqrt{3}}$ and the corresponding value of x is $x_c = \sqrt{3}$. Thus (1.76) applies while $t < t_c$, and thereafter the solution also applies in $x < x_S(t)$ and $x > x_S(t)$, where

$$\dot{x}_S = \tfrac{1}{2}[u(x_S+) + u(x_S-)], \tag{1.79}$$

with

$$x_S = \sqrt{3} \quad \text{at} \quad t = \frac{8}{3\sqrt{3}}. \tag{1.80}$$

As indicated in figure 1.16, the characteristics intersect at the shock, and it is geometrically clear from figure 1.14, for example, that u_+ and u_- are the largest and smallest roots of the cubic (1.76). An explicit solution for x_S is not readily available, but it is of interest to establish the long term behaviour, and for this we need approximations to the roots of (1.76) when $t \gg 1$.

We write the cubic (1.76) in the form

$$u = \frac{x}{t} \pm \frac{1}{t}\left(\frac{1-u}{u}\right)^{1/2}. \tag{1.81}$$

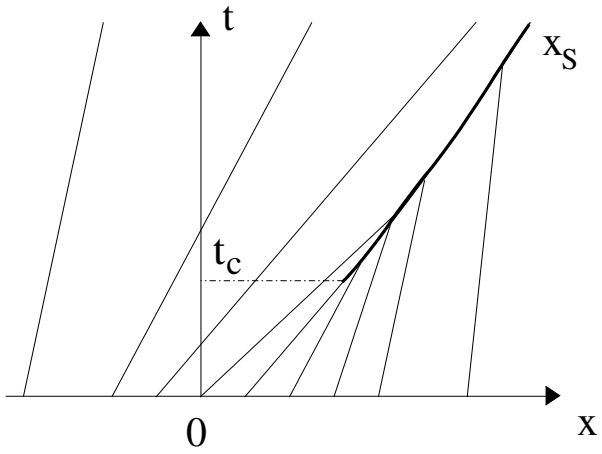

Figure 1.16: Characteristic diagram indicating shock formation.

We know that $u \leq 1$, and we expect x_S to tend to infinity as $t \to \infty$, so that we suppose $x \gg 1$. In that case $u \approx x/t$ if $u = O(1)$, and the next corrective term gives

$$u \approx \frac{x}{t} \pm \frac{1}{t}\left(\frac{t-x}{x}\right)^{1/2}. \tag{1.82}$$

This evidently gives the upper two roots for $x < t$ (since they coalesce at $u = 1$ when $x = t$). For large x, the other root must have $u \ll 1$, and in fact

$$u \approx \frac{1}{x^2}, \tag{1.83}$$

in order that (1.81) not imply (1.82).[3] Alternatively, (1.83) follows from consideration of (1.76) in the form

$$t^2u^3 - 2xtu^2 + (x^2+1)u - 1 = 0, \tag{1.84}$$

providing $x \gg t^{1/3}$.

To find the location of the 'noses' of the solution, we note that the approximation that $u \approx x/t$ breaks down (see (1.82)) when $x \sim t^{1/3}$, which is also where (1.83) becomes invalid. This suggests writing

$$u = \frac{x}{t}W(X), \quad X = \frac{x}{t^{1/3}}, \tag{1.85}$$

and then $W(X)$ is given approximately, for large t, by

$$W(W-1)^2 = \frac{1}{X^3}, \tag{1.86}$$

and for $X = O(1)$ there are three roots providing $X > 3/2^{2/3}$; at $X = 3/2^{2/3}$, the two lower roots coalesce at $W = \frac{1}{3}$: this describes the left nose of the curve.

[3] We need $u \lesssim O\left(\frac{1}{x^2}\right)$ in order that the second term in (1.81) be significant (otherwise we regain (1.82)), and in fact we need the two terms to be approximately equal, so that $0 < u < 1$: hence (1.83).

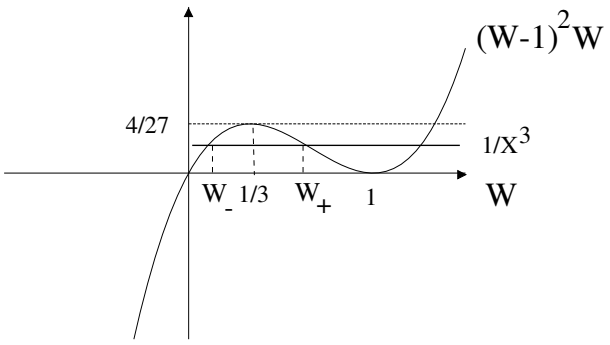

Figure 1.17: Determination of $W(X)$.

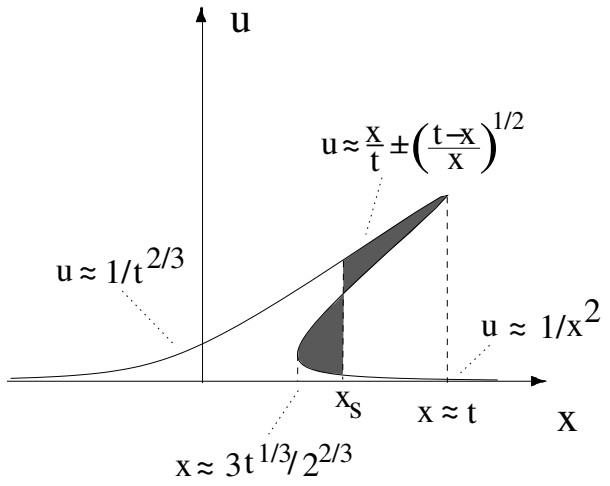

Figure 1.18: Large time solution of the characteristic solution.

As X becomes large, the upper two roots approach $W = 1$, thus $u \approx x/t$, while the lower approaches zero, specifically $W \approx 1/X^3$, and hence $u \approx 1/x^2$: see figure 1.17. Thus these roots match to the approximations in (1.82) and (1.83). As X becomes small, the remaining root is given by $W \approx 1/X$, so that $u \approx 1/t^{2/3}$, and (1.84) shows that this is the correct approximation as long as $|x| \ll t^{1/3}$. The situation is shown in figure 1.18).

In order to determine the shock location x_S, we make the ansatz that $t^{1/3} \ll x_S \ll t$, i. e., that the shock is far from both noses. In that case

$$u_+ \approx \frac{1}{x_S^2}, \quad u_- \approx \frac{x_S}{t}, \tag{1.87}$$

and at leading order we have

$$\dot{x}_S \approx \frac{x_S}{2t}, \tag{1.88}$$

whence

$$x_S \approx at^{1/2}, \tag{1.89}$$

confirming our assumption that $t^{1/3} \ll x_S \ll t$.

To determine the coefficient a, we may use the equal area rule, which follows from conservation of mass, and states that the two shaded areas in figure 1.18 cut off by the shock are equal. We use (1.85) for the left hand area, and (1.82) for the right hand area. Then

$$\int_{3t^{1/3}/2^{2/3}}^{at^{1/2}} \frac{x}{t}\left[W_+(X) - W_-(X)\right]\, dx \approx \int_{at^{1/2}}^{t} \frac{2}{t}\left(\frac{t-x}{x}\right)^{1/2} dx, \tag{1.90}$$

where W_+ and W_- are the middle and lowest roots of (1.86), as shown in figure 1.17. We write $x = t^{1/2}\xi$ in the left integral and $x = t\eta$ in the right, and hence we deduce that

$$a \approx \int_0^1 2\left(\frac{1-\eta}{\eta}\right)^{1/2} d\eta = \pi. \tag{1.91}$$

1.4.2 Burgers' equation

Although the presence of a shock for (1.71) is entirely consistent with the derivation of the equation from an integral conservation law, nature appears generally to avoid discontinuities and singularities, and it is usually the case that in writing an equation such as (1.71), we have neglected some term which acts to smooth the shock, so that the change of u is rapid but not abrupt.

The most common type of neglected term which provides the necessary smoothing is a diffusion term, which is manifested in the adjusted equation as a second derivative term. The resulting equation is known as Burgers' equation:

$$u_t + uu_x = \kappa u_{xx}. \tag{1.92}$$

Sometimes, as for example in the smoothing effect of heat conduction or viscosity on sonic shock waves, such a term genuinely represents a physically diffusive process (e. g., diffusion of heat or momentum); sometimes it arises for more subtle reasons, as for example in the smoothing of waves on rivers (see, for example, the derivation of equation (4.57) in the discussion of the monoclinal flood wave in chapter 4).

More generally, even-order derivative terms of the form $(-1)^{n-1}\kappa\dfrac{\partial^{2n}u}{\partial x^{2n}}$ are smoothing. (This can be seen by the fact that solutions of the resulting linearised equation $u_t = (-1)^{n-1}\kappa\dfrac{\partial^{2n}u}{\partial x^{2n}}$ have damped solutions $\exp(ikx + \sigma t)$ in which $\sigma = -\kappa k^{2n}$.) A fourth order smoothing term occurs in the smoothing of capillary waves by surface tension, for example.

How does the presence of a diffusive term modify the structure of the solutions? If κ is small, we should suppose that it has little effect, so that shocks would start to form. However, the neglect of the diffusion term becomes invalid when the derivatives of u become large. In fact, the diffusion term is trying to do the opposite of

the advective term. The latter is trying to fold the initial profile together like an accordion, while the former is trying to spread everything apart. We might guess that a balanced position is possible, in which the nonlinear advective term keeps the profile steep, but the diffusion prevents it actually folding over (and hence causing a discontinuity), and this will turn out to be the case.

Shock structure

We suppose $\kappa \ll 1$, so that $u_t + uu_x \approx 0$, and a shock forms at $x = x_S(t)$. Our aim is to show that (1.92) supports a *shock structure*, i. e., a region of rapid change for u near x_S from u_- to u_+.

To focus on the shock, we need to rescale x near x_S, and we do this by writing

$$x = x_S(t) + \kappa X. \tag{1.93}$$

Burgers' equation becomes

$$\kappa u_t - \dot{x}_S u_X + uu_X = u_{XX}. \tag{1.94}$$

We expect the characteristic solution (with $\kappa = 0$) to be approximately valid far from x_S, and so appropriate conditions (technically, these are *matching conditions*) are

$$u \to u_\pm \ \text{ as } \ X \to \pm\infty, \tag{1.95}$$

and we take these values as prescribed from the *outer* solution (i. e., the solution of $u_t + uu_x = 0$ as $x \to x_S\pm$).

Since $\kappa \ll 1$, (1.94) suggests that u relaxes rapidly (on a time scale $t \sim \kappa \ll 1$) to a quasi-steady state (quasi-steady, because u_+ and u_- will vary with t) in which

$$-\dot{x}_S u_X + uu_X \approx u_{XX}, \tag{1.96}$$

whence

$$K - \dot{x}_S u + \tfrac{1}{2}u^2 \approx u_X, \tag{1.97}$$

and prescription of the boundary conditions implies

$$K = \dot{x}_S u_+ - \tfrac{1}{2}u_+^2 = \dot{x}_S u_- - \tfrac{1}{2}u_-^2, \tag{1.98}$$

whence

$$\dot{x}_S = \frac{[\frac{1}{2}u^2]_-^+}{[u]_-^+}, \tag{1.99}$$

which is precisely the jump condition we obtained in (1.74). The solution for u of (1.97) is then

$$u = c - (u_- - c)\tanh\left[\tfrac{1}{2}(u_- - c)X\right], \tag{1.100}$$

where $c = \dot{x}_S$.

1.4.3 The Fisher equation

In Burgers' equation, a wave arises as a balance between nonlinear advection and diffusion. In Fisher's equation,

$$u_t = u(1-u) + u_{xx}, \tag{1.101}$$

a wave arises as a mechanism for transferring a variable from an unstable steady state ($u = 0$) to a stable one ($u = 1$). Whereas Burgers' equation balances two transport terms, Fisher's equation balances diffusive transport with an algebraic source term. It originally arose as a model for the dispersal of an advantageous gene within a population, and has taken a plenary rôle as a pedagogical example in mathematical biology of how reaction (source terms) and diffusion can combine to produce travelling waves.

We pose (1.101) with boundary conditions

$$\begin{aligned} u &\to 1, \quad x \to -\infty, \\ u &\to 0, \quad x \to +\infty. \end{aligned} \tag{1.102}$$

It is found (and can be proved) that any initial condition leads to a solution which evolves into a travelling wave of the form

$$u = f(\xi), \quad \xi = x - ct, \tag{1.103}$$

where

$$f'' + cf' + f(1-f) = 0, \tag{1.104}$$

and

$$f(\infty) = 0, \quad f(-\infty) = 1. \tag{1.105}$$

In the (f, g) phase plane, where $g = -f'$, we have

$$\begin{aligned} f' &= -g, \\ g' &= f(1-f) - cg, \end{aligned} \tag{1.106}$$

and a travelling wave corresponds to a trajectory which moves from (1,0) to (0,0).

Linearisation of (1.106) near the fixed point $(f^*, 0)$ via $f = f^* + F$ leads to

$$\begin{pmatrix} F \\ g \end{pmatrix}' = \begin{pmatrix} 0 & -1 \\ 1 - 2f^* & -c \end{pmatrix} \begin{pmatrix} F \\ g \end{pmatrix}, \tag{1.107}$$

with solutions $e^{\lambda\xi}$, where $\lambda^2 + c\lambda + (1 - 2f^*) = 0$. We anticipate $c > 0$; then $(1, 0)$ is a saddle point, while $(0, 0)$ is a stable node if $c \geq 2$ (and a spiral if $c < 2$). For $c \geq 2$, a connecting trajectory exists as shown in figure 1.19: in practice the minimum wave speed $c = 2$ is selected. (Connecting trajectories also exist if $c < 2$, but because (0,0) is a spiral, these have oscillating tails as $u \to 0$, which are unstable and also (for example, if u represents a population) unphysical.)

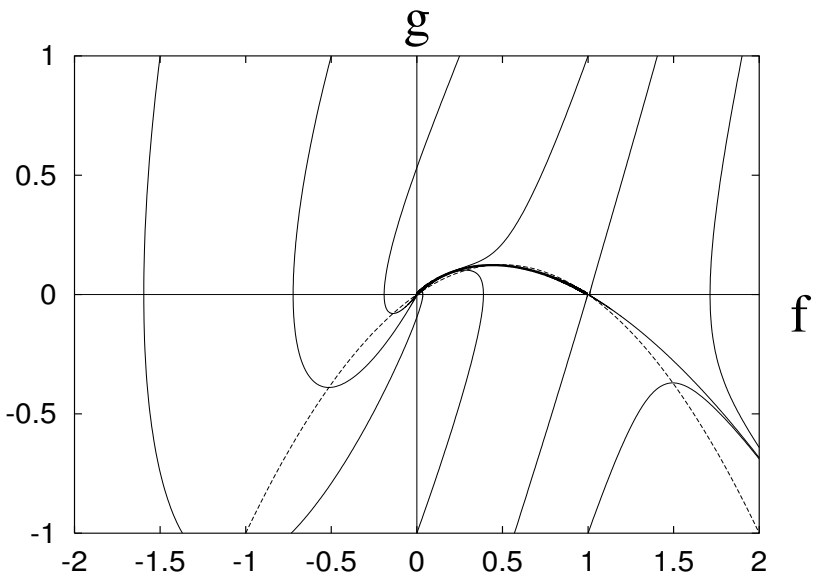

Figure 1.19: Phase portrait of Fisher equation, (1.106), for $c = 2$. Note how close the connecting trajectory (thick line) is to the g nullcline. This is why the large c approximation is accurate *for this trajectory*.

Explicit solutions for (1.104) are not available, but an excellent approximation is easily available. We put

$$\xi = c\Xi, \tag{1.108}$$

so

$$\nu f'' + f' + f(1-f) = 0, \tag{1.109}$$

with $\nu = 1/c^2 = 1/4$ for $c = 2$. Taking $\nu \ll 1$ and writing $f = f_0 + \nu f_1 + \ldots$, we have

$$\begin{aligned} f_0' + f_0(1-f_0) &= 0, \\ f_1' + (1-2f_0)f_1 &= -f_0'', \end{aligned} \tag{1.110}$$

and thus

$$f_0 = \frac{e^{-\Xi}}{1+e^{-\Xi}}. \tag{1.111}$$

Also, noting that $1 - 2f_0 = -f_0''/f_0'$ (differentiate $(1.110)_1$),

$$f_1 = f_0(1-f_0)\ln[f_0(1-f_0)], \tag{1.112}$$

and so on. Even the first term gives a good approximation, and even for $c = 2$.

1.4.4 Solitons

The Fisher wave is an example of a solitary travelling wave. Another type of solitary wave is the soliton, as exemplified by solutions of the Korteweg-de Vries equation

$$u_t + uu_x + u_{xxx} = 0. \tag{1.113}$$

This has travelling wave solutions $u = f(\xi)$, $\xi = x - ct$, where

$$f''' + ff' - cf' = 0, \tag{1.114}$$

and solitary waves with $f \to 0$ at $\pm\infty$ satisfy the first integral

$$f'' + \tfrac{1}{2}f^2 - cf = 0, \tag{1.115}$$

and thus

$$\tfrac{1}{2}f'^2 + \tfrac{1}{6}f^3 - \tfrac{1}{2}cf^2 = 0, \tag{1.116}$$

with solution

$$f = \tfrac{3}{2}c\ \mathrm{sech}^{\,2}\left(\frac{\sqrt{c}\,\xi}{2}\right). \tag{1.117}$$

Thus there is a one parameter family of these solitary waves, and they are called solitons, because they have the remarkable particle-like ability to 'pass through' each other without damage, except for a change of relative phase. Despite the nonlinearity, they obey a kind of superposition principle. Soliton equations (of which there are many) have many other remarkable properties, beyond the scope of the present discussion.

Some understanding of the solitary wave arises through an understanding of the balance between nonlinearity (uu_x) and dispersion (u_{xxx}). The dispersive part of the equation, $u_t + u_{xxx} = 0$, is so called because waves $\exp[ik(x - ct)]$ have wave speed $c = -k^2$ which depends on wavenumber k; waves of different wavelengths $(2\pi/k)$ move at different speeds and thus disperse. On the other hand, the nonlinear advection equation $u_t + uu_x$ has a focussing effect, which (from a spectral point of view) concentrates high wave numbers near shocks (rapid change means large derivatives means high wavenumber). So the nonlinearity tries to move high wavenumber modes in from the left, while the dispersion tries to move them to the left: again a balance is struck, and a travelling wave is the result.

1.4.5 Nonlinear diffusion: similarity solutions

Like travelling wave solutions, similarity solutions are important indicators of solution behaviour. A particularly illuminating illustration of this behaviour is provided by the general nonlinear diffusion equation

$$u_t = (u^m u_x)_x, \tag{1.118}$$

which arises in many contexts. We shall illustrate the derivation of this equation for a fluid droplet below. Typically, (1.118) represents the conservation of the density of some quantity u with a diffusive flux $-u^m u_x$. A standard kind of problem to consider is then the release of a concentrated amount at $x = 0$ at $t = 0$. We can idealise this by supposing that at $t = 0$ (in suitable units),

$$u = 0 \text{ for } x \neq 0, \quad \int_{-\infty}^{\infty} u(x)\,dx = 1. \tag{1.119}$$

This apparently contradictory prescription idealises the concept of a very concentrated local injection of u. For example, (1.118) with (1.119) could represent the diffusion of sugar in hot (one-dimensional) tea from an initially emplaced sugar grain. (1.119) defines the delta function $\delta(x)$, an example of a generalised function. One can think of generalised functions as being (defined by) the equivalence classes of well-behaved functions u_n with appropriate limiting behaviour. For example, the delta function is defined by the class of well-behaved functions u_n for which

$$\int_{-\infty}^{\infty} u_n(x) f(x)\, dx \to f(0) \tag{1.120}$$

as $n \to \infty$ for all well-behaved $f(x)$. As a shorthand, then,

$$\int_{-\infty}^{\infty} \delta(x) f(x)\, dx = f(0) \tag{1.121}$$

for any f, but the ulterior definition is really in (1.120). In practice, however, we think of a delta function as a 'function' of x, zero everywhere except for a (very) sharp spike at $x = 0$.

In solving (1.118), we also apply boundary conditions

$$u \to 0 \quad \text{as} \quad x \to \pm\infty, \tag{1.122}$$

and these, together with the equation and initial condition, imply that

$$\int_{-\infty}^{\infty} u\, dx = 1 \tag{1.123}$$

for all time.

A similarity solution is appropriate because there are no intrinsic space or time scales for the problem. It is in this context that one can expect the solution to look the same at different times on different scales. In general, as t varies, then the length scale might vary as $\xi(t)$ and the amplitude of the solution u might vary as $U(t)$. That is, if we look at u/U as a function of x/ξ, it will look the same for all t. This in turn implies that the solution takes the form

$$u = U(t) f\left[\frac{x}{\xi(t)}\right], \tag{1.124}$$

and this is one of the forms of a similarity solution.

It is often the case that U and ξ are powers of t, and the exponents are to be chosen so that the problem has such a solution. This is best seen by example. If we denote $\eta = x/\xi(t)$, and substitute the form (1.124) into (1.118), (1.122) and (1.123), we find

$$\frac{U'}{U} f - \frac{\xi'}{\xi} \eta f' = \frac{U^m}{\xi^2} [f^m f']', \tag{1.125}$$

where $U' = dU/dt$, $\xi' = d\xi/dt$, but $f' = df/d\eta$. The initial/boundary conditions become

$$f(\pm\infty) = 0, \tag{1.126}$$

and the normalisation condition (1.123) is

$$U\xi \int_{-\infty}^{\infty} f \, d\eta = 1. \tag{1.127}$$

A solution can be found provided the t dependence vanishes from the model, and this requires $U\xi = 1$ (the constant can be taken as one without loss of generality), whence (1.125) becomes

$$[f^m f']' + \xi^{m+1}\xi'(\eta f)' = 0, \tag{1.128}$$

and $\xi^{m+1}\xi'$ must be constant. It is algebraically convenient to choose $\xi^{m+1}\xi' = 2/m$, thus

$$\eta = x\left[\frac{m}{2(m+2)t}\right]^{\frac{1}{m+2}}, \tag{1.129}$$

and a first integral of (1.128) is

$$f^m f' + \frac{2}{m}\eta f = 0, \tag{1.130}$$

with the constant of integration being zero (because $f \to 0$ as $\eta \to \pm\infty$). Thus either $f = 0$, or

$$f = [\eta_0^2 - \eta^2]^{1/m}, \tag{1.131}$$

so that the solution has the form of a cap of finite extent, given by (1.131) (for $|\eta| < \eta_0$, and $f = 0$ for $|\eta| > \eta_0$. The value of η_0 is determined from $\int_{-\infty}^{\infty} f \, d\eta = 1$, and is

$$\eta_0 = \frac{1}{\left[2\int_0^{\pi/2} \cos^{\frac{m+2}{m}}\theta d\theta\right]^{\frac{m}{m+2}}}. \tag{1.132}$$

The finite extent of the profile is due to the degeneracy of the equation when $m > 0$. (The limit $m \to 0$ regains the Gaussian solution of the heat equation by first putting $\eta = \sqrt{m}\eta_0\zeta$, $f = F/\sqrt{m}$, and noting that $\eta_0 \approx (\pi m)^{-m/2}$ as $m \to 0$ (this last following by application of Laplace's method to (1.132)).) The graph of $f(\eta)$ is shown in figure 1.20.

1.4.6 The viscous droplet

An example of where the nonlinear diffusion equation can arise is in the dynamics of a drop of viscous fluid on a level surface. If the fluid occupies the region $0 < z < h(x, y, t)$ and is shallow, then lubrication theory gives the approximation

$$\begin{aligned} \boldsymbol{\nabla} p &= \mu \frac{\partial^2 \mathbf{u}}{\partial z^2}, \\ p_z &= -\rho g, \end{aligned} \tag{1.133}$$

in which $\mathbf{u} = (u, v, 0)$ is the horizontal component of velocity, and $\boldsymbol{\nabla}$ is the horizontal gradient $(\partial/\partial x, \partial/\partial y, 0)$. With $p = 0$ at $z = h$, we have the hydrostatic pressure

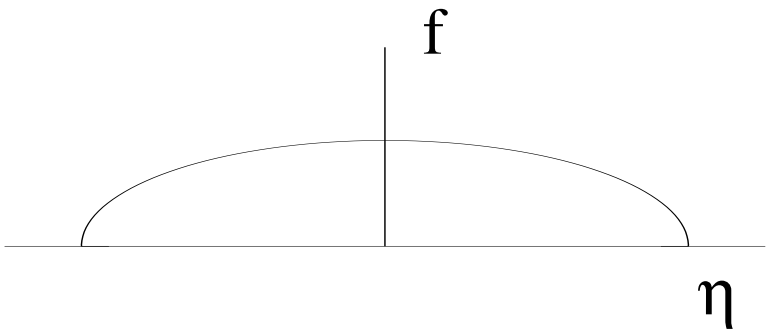

Figure 1.20: $f(\eta)$ given by (1.131).

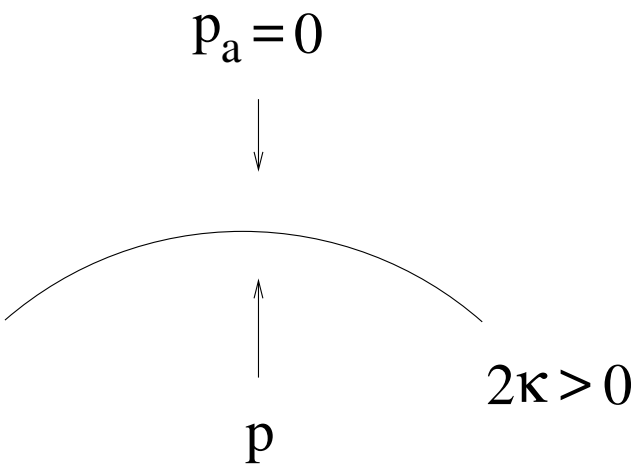

Figure 1.21: The surface shown has positive curvature when the radius of curvature is measured from below the surface; in this case equilibrium requires $p > p_a$.

$p = \rho g(h - z)$, so that $\boldsymbol{\nabla} p = \rho g \boldsymbol{\nabla} h$, and three vertical integrations of $(1.133)_1$ (with zero shear stress $\partial \mathbf{u}/\partial z = 0$ at $z = h$ and no slip $\mathbf{u} = 0$ at $z = 0$) yield the horizontal fluid flux

$$\mathbf{q} = \int_0^h \mathbf{u}\, dz = -\frac{\rho g}{3\mu} h^2 \boldsymbol{\nabla} h. \tag{1.134}$$

Conservation of fluid volume for an incompressible fluid is $h_t + \boldsymbol{\nabla}.\mathbf{q} = 0$, and thus

$$h_t = \frac{\rho g}{3\mu} \boldsymbol{\nabla}.[h^3 \boldsymbol{\nabla} h], \tag{1.135}$$

corresponding to (1.118) (in two space dimensions) with $m = 3$. A drop of fluid placed on a table will spread out at a finite rate.

That this does not continue indefinitely is due to surface tension. Rather than having $p = 0$ at $z = h$ (where the atmospheric pressure above is taken as zero), the effect of surface tension is to prescribe

$$p = 2\gamma\kappa, \tag{1.136}$$

where γ is the surface tension, and κ is the mean curvature relative to the fluid droplet (i. e., $\kappa > 0$ if the interface is concave[4], as illustrated in figure 1.21). The curvature is defined as $2\kappa = \boldsymbol{\nabla}.\mathbf{n}$, where $\mathbf{n}$ is the unit normal pointing away from the fluid (i. e., upwards). At least this shorthand definition works if we define

$$\mathbf{n} = \frac{(-h_x, -h_y, 1)}{[1 + |\boldsymbol{\nabla} h|^2]^{1/2}}; \tag{1.137}$$

thus

$$2\kappa = -\boldsymbol{\nabla}. \left[\frac{\boldsymbol{\nabla} h}{\{1 + |\boldsymbol{\nabla} h|^2\}^{1/2}} \right]. \tag{1.138}$$

It is less obvious that it will work more generally, since there are many ways of defining the interface in the form $\phi(x, y, z) = 0$ and thus $\mathbf{n} = \boldsymbol{\nabla}\phi/|\boldsymbol{\nabla}\phi|$ (that in (1.137) uses $\phi = z - h$); but in fact it does not matter, since we may generally take $\phi = (z - h)P$ for some arbitrary smooth function P, so that $\boldsymbol{\nabla}\phi = (-h_x, -h_y, 1)P$ on $z = h$, and $\boldsymbol{\nabla}\phi/|\boldsymbol{\nabla}\phi|$ is the same expression as in (1.137).

For shallow flows, we replace $p = 0$ on $z = h$ by $p = -\gamma\nabla^2 h$ there, and thus

$$p \approx \rho g(h - z) - \gamma\nabla^2 h, \tag{1.139}$$

and (via (1.134)), (1.135) is modified to

$$h_t = \boldsymbol{\nabla}. \left[\frac{h^3}{3\mu} \boldsymbol{\nabla}\{\rho g h - \gamma\nabla^2 h\} \right]. \tag{1.140}$$

The fourth order term is also 'diffusive', insofar as it is a smoothing term, as already mentioned: high wave number (high gradient) modes are rapidly damped. The effect of surface tension relative to the diffusional gravity term is given by the Bond number

$$Bo = \frac{\rho g l^2}{\gamma}, \tag{1.141}$$

where l is the lateral length scale of the drop. This is the (only) dimensionless parameter which occurs when (1.140) is written dimensionlessly.

1.4.7 Advance and retreat: waiting times

The similarity solution (1.131) predicts an infinite slope at the margin (where $f = 0$) if $m > 1$ (and a zero slope if $m < 1$). If one releases a finite quantity at $t = 0$, then one expects the long time solution to be this similarity solution. The question then arises as to how this similarity solution is approached, in particular if the initial droplet has finite slope at the margin.

This question can be addressed in a more general way by studying the behaviour near the margin $x = x_S(t)$ of a solution $h(x, t)$ of (1.118),

$$h_t = (h^m h_x)_x. \tag{1.142}$$

[4]Geomorphologists would call this surface convex; see chapter 6.

Suppose that $h \sim c(x_S - x)^\nu$ for x near x_S. Then satisfaction of (1.142) requires

$$\dot{x}_S \approx c^m[\nu(m+1) - 1](x_S - x)^{\nu m - 1}. \tag{1.143}$$

Note that the similarity solution (1.131) has $\dot{x}_S$ finite when $\nu = 1/m$, consistent with (1.143), and more generally we see that the margin will advance at a rate $\dot{x}_S \approx c^m/m$ if $h \sim c(x_S - x)^{1/m}$.

Suppose now that $m > 1$, and we emplace a droplet with finite slope, $\nu = 1$. Then the right hand side of (1.143) is zero at $x = x_S$, and thus $\dot{x}_S = 0$: the front does not move. What happens in this case is that the drop flattens out: there is transport of h towards the margin, which steepens the slope at x_S until it becomes infinite, at which point it will move. This pause while the solution fattens itself prior to margin movement is called a *waiting time*.

Conversely, if $m < 1$, then the front moves (forward) if the slope is zero there, and $\nu = 1/m$. If the slope is finite, $\nu = 1$, then (1.143) would imply infinite speed. An initial drop of finite margin slope will instantly develop zero front slope as the margin advances.

(1.143) does not allow the possibility of retreat, because it describes a purely diffusive process. The possibility of both advance and retreat is afforded by a model of a viscous droplet with accretion, one example of which is the mathematical model of an ice sheet.[5] Essentially, an ice sheet, such as that covering Antarctica or Greenland, can be thought of as a (large) viscous droplet which is nourished by an accumulation rate (of ice formed from snow). A general model for such a nourished droplet is

$$h_t = (h^m h_x)_x + a, \tag{1.144}$$

where a represents the accumulation rate. Unlike the pure diffusion process, (1.144) has a steady state

$$h = \left[\tfrac{1}{2}(m+1)a(x_0^2 - x^2)\right]^{1/(m+1)}, \tag{1.145}$$

where x_0 must be prescribed. (In the case of an ice sheet, we might take x_0 to be at the continental margin.) (1.145) is slightly artificial, as it requires $a = 0$ for $x > x_0$, and allows a finite flux $-h^m h_x = a x_0$ where $h = 0$. More generally, we might allow accumulation and ablation (snowfall and melting), and thus $a = a(x)$, with $a < 0$ for large $|x|$. In that case the steady state is

$$h = \left[(m+1)\int_x^{x_0} s\,dx\right]^{1/(m+1)}, \tag{1.146}$$

where the balance function s is

$$s = \int_0^x a\,dx, \tag{1.147}$$

and x_0 is defined to be where accumulation balances ablation,

$$\int_0^{x_0} a\,dx = 0. \tag{1.148}$$

[5]Ice sheets and their marginal movement are discussed further in chapter 10.

This steady state is actually stable, and both advance and retreat can occur. Suppose the margin is at x_S, where $a = a_S = -|a_S|$ ($a_S < 0$, representing ablation). If we put $h \approx c(x_S - x)^\nu$, then (1.144) implies

$$\nu c \dot{x}_S (x_S - x)^{\nu-1} \approx \nu c^{m+1}[\nu(m+1) - 1](x_S - x)^{[\nu(m+1)-2]} - |a_S|, \tag{1.149}$$

and there are three possible balances of leading order terms.

The first is as before,

$$\dot{x}_S \approx c^m[\nu(m+1) - 1](x_S - x)^{\nu m - 1}, \tag{1.150}$$

and applies generally if $\nu < 1$. Supposing $m > 1$, then we have advance, $\dot{x}_S \approx c^m/m$ if $\nu = 1/m$, but if $\nu > 1/m$, this cannot occur, and the margin is stationary if $1/m < \nu < 1$. If $\nu = 1$, then $\nu(m+1) - 2 = m - 1 > 0$, so that

$$\dot{x}_S \approx -|a_S|/c, \tag{1.151}$$

and the margin retreats; if $\nu > 1$, then instantaneous adjustment to finite slope and retreat occurs.

The ice sheet exhibits the same sort of waiting time behaviour as the viscous droplet without accretion. For $1/m < \nu < 1$, the margin is stationary, and if $x_S < x_0$ then the margin slope will steepen until $\nu = 1/m$, and advance occurs. On the other hand, if $x_S > x_0$, then the slope will decrease until $\nu = 1$, and retreat occurs. In the steady state, a balance is achieved (from (1.146)) when $\nu = 2/(m+1)$.

1.4.8 Blow-up

Further intriguing possibilities arise when the source term is nonlinear. An example is afforded by the nonlinear (reaction-diffusion) equation

$$u_t = u_{xx} + \lambda e^u, \tag{1.152}$$

which arises in the theory of combustion. Indeed, as we saw earlier, combustion occurs through the fact that multiple steady states can exist for a model such as (1.30), and the same is true for (1.152), which can have two steady solutions. In fact, if we solve $u'' + \lambda e^u = 0$ with boundary conditions $u = 0$ on $x = \pm 1$, then the solutions are

$$u = 2 \ln \left[A \operatorname{sech} \left\{ \sqrt{\frac{\lambda}{2}} A x \right\} \right], \tag{1.153}$$

where $A = \exp[u(0)/2]$, and A satisfies

$$A = \cosh \left[\sqrt{\frac{\lambda}{2}} A \right], \tag{1.154}$$

which has two solutions if $\lambda < 0.878$, and none if $\lambda > 0.878$: the situation is depicted in figure 1.22. If we replace e^u by $\exp[u/(1 + \varepsilon u)]$, $\varepsilon > 0$, we regain the top (hot) branch also, as in figure 1.9.

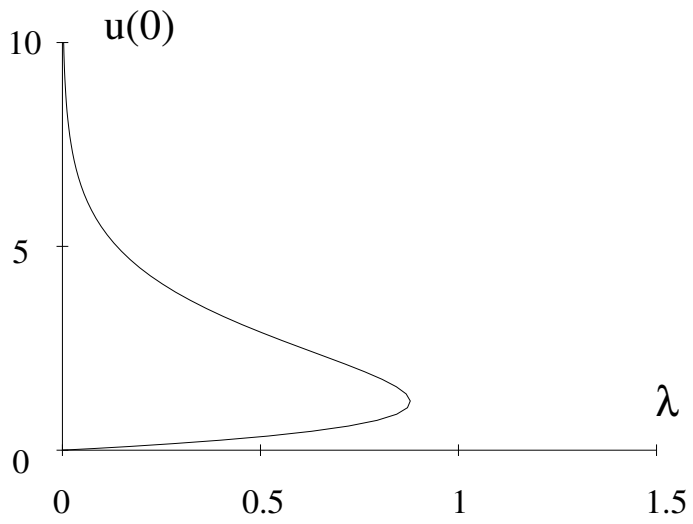

Figure 1.22: Maximum value of steady solutions u of (1.152), $u(0)$, as a function of the parameter λ. Blow-up occurs if $\lambda \gtrsim 0.878$.

One wonders what the absence of a steady state for (1.152) if $\lambda > \lambda_c$ implies. The time-dependent problem certainly has a solution, and an idea of its behaviour can be deduced from the spatially independent problem, $u_t = \lambda e^u$, with solution $u = \ln[1/\{\lambda(t_0 - t)\}]$: u reaches infinity in a finite time. This phenomenon is known as *thermal runaway*, and more generally the creation of a singularity of the solution in finite time is called *blow-up*. Numerical solutions of the equation (1.152) including the diffusion term show that blow-up still occurs, but at an isolated point; figure 1.23 shows the approach to blow-up as t approaches a critical blow-up time t_c.

In fact, one can prove generally that no steady solutions exist for λ greater than some critical value, and also that in that case, blow-up will occur in finite time. To do this, we use some slightly more sophisticated mathematics.

Suppose we want to solve the more general problem

$$u_t = \nabla^2 u + \lambda e^u \quad \text{in} \quad \Omega, \tag{1.155}$$

with $u = 0$ in the boundary $\partial\Omega$, and $u = 0$ at $t = 0$ (these conditions are for convenience rather than necessity). We will be able to prove results for (1.155) which are comparable to those for the ordinary differential equation version (cf. (1.33))

$$\dot{w} = -\mu_1 w + \lambda e^w, \tag{1.156}$$

because, in some loose sense, the Laplacian operator ∇^2 resembles a loss term.

More specifically, we recall some pertinent facts about the (Helmholtz) eigenvalue problem

$$\nabla^2 \phi + \mu\phi = 0 \quad \text{in} \quad \Omega, \tag{1.157}$$

with $\phi = 0$ on $\partial\Omega$. There exists a denumerable sequence of real eigenvalues $0 < \mu_1 \leq \mu_2 \ldots$, with $\mu_n \to \infty$ as $n \to \infty$, and corresponding (real) eigenfunctions $\phi_1, \phi_2, ...$

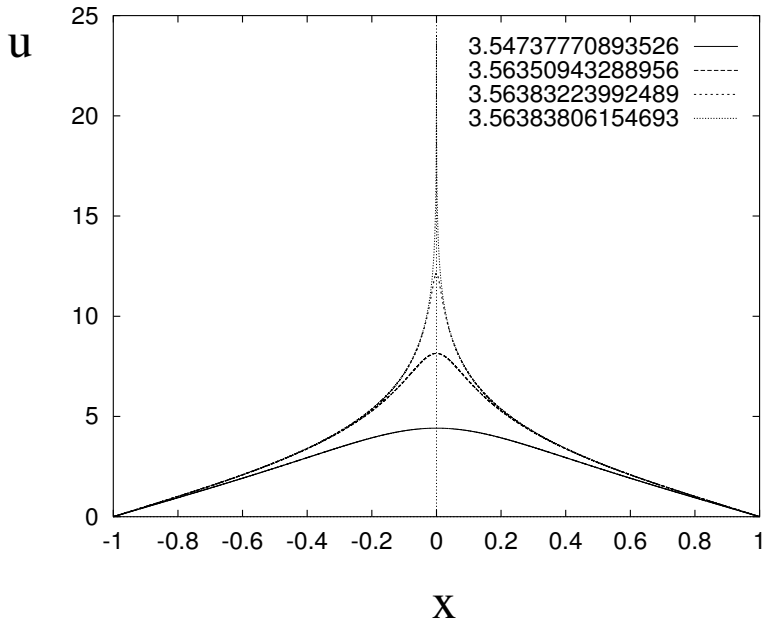

Figure 1.23: Solution of $u_t = u_{xx} + e^u$ on $[-1, 1]$, with $u = 0$ at $x = -1, 1$ and $t = 0$. The solution is shown for four times close to the blow-up time, which in this computation is $t_c = 3.56384027594971$. The many decimal places indicate the logarithmic suddenness of the runaway as $t \to t_c$, but the value of t_c itself will depend on the numerical approximation used.

which form an orthonormal set (using the L^2 norm), thus

$$(\phi_i, \phi_j) \equiv \int_\Omega \phi_i \phi_j \, dV = \delta_{ij}, \tag{1.158}$$

where δ_{ij} is the Kronecker delta ($= 1$ if $i = j$, 0 if $i \neq j$). These eigenvalues satisfy a variational principle of the form

$$\mu_i = \min \int_\Omega |\boldsymbol{\nabla}\phi|^2 \, dV, \tag{1.159}$$

where ϕ ranges over functions of unit norm, $\|\phi\|_2 = \{\int \phi^2 \, dV\}^{1/2} = 1$, which are orthogonal to ϕ_j for $j < i$; (more generally $\mu_i = \min\left\{\int |\boldsymbol{\nabla}\phi|^2 \, dV / \int \phi^2 \, dV\right\}$ if ϕ is not normalised on to the unit sphere $\|\phi\|_2 = 1$). In particular

$$\mu_1 = \min_{\|\phi\|_2 = 1} \int_\Omega |\boldsymbol{\nabla}\phi|^2 dV, \tag{1.160}$$

and the corresponding ϕ_1 is of one sign, let us say positive.

We take the inner product of the equation (1.155) with ϕ_1 and divide by $\int \phi_1 \, dV$; defining

$$v(t) = \frac{\int_\Omega u\phi_1 \, dV}{\int_\Omega \phi_1 \, dV} = \int_\Omega u \, d\omega, \tag{1.161}$$

where $d\omega = \phi_1\, dV / \int_\Omega \phi_1\, dV$ is a measure on Ω (with $\int_\Omega d\omega = 1$), and using Green's theorem, we find

$$\dot{v} = \lambda \int_\Omega e^u\, d\omega - \mu_1 v, \tag{1.162}$$

and the equation for v is close to the ordinary differential equation (1.156).

Now we use Jensen's inequality. This says that if we have an integrable function $g(\mathbf{x})$ on Ω and a convex function $f(s)$ on $\mathbf{R}$ (i. e., one that bends upwards, $f'' > 0$), then

$$f\left[\int_\Omega g(\mathbf{x})\, d\omega\right] \leq \int_\Omega f[g(\mathbf{x})]\, d\omega \tag{1.163}$$

for any measure ω on Ω such that $\int_\Omega d\omega = 1$. We have chosen ω to be so normalised, and e^u is convex: thus

$$\int_\Omega \exp(u)\, d\omega \geq \exp\left[\int_\Omega u\, d\omega\right] = e^v, \tag{1.164}$$

so that

$$\dot{v} \geq \lambda e^v - \mu_1 v. \tag{1.165}$$

It is now easy to prove non-existence of steady states and blow-up for λ greater than some critical value λ_c. Firstly, u must be positive, and hence also v. (For suppose $u < 0$: since $u = 0$ at $t = 0$ and on $\partial\Omega$, then u attains its minimum in Ω at some $t > 0$, at which point $u_t \leq 0$, $u_{xx} \geq 0$, which is impossible, since then $u_t - u_{xx} = \lambda e^u \leq 0$.) For any v, $e^v \geq ev$, thus $\dot{v} \geq (\lambda e - \mu_1)v$. In a steady state we must have $\dot{v} = 0$, and also $v > 0$ (since clearly $u = 0$ is not a steady solution), and this pair of conditions is impossible if

$$\lambda > \mu_1 / e. \tag{1.166}$$

This implies non-existence of a steady solution for $\lambda > \lambda_c$, where $\lambda_c \leq \mu_1/e$.

In a similar vein, if $\lambda > \mu_1/e$, then

$$\dot{v} > \mu_1[e^{v-1} - v], \tag{1.167}$$

and $v > w$, where

$$\dot{w} = \mu_1(e^{w-1} - w), \quad w(0) = 0. \tag{1.168}$$

(This is a standard comparison argument: $v = w$ at $t = 0$, and $\dot{v} > \dot{w}$ there, so $v - w$ is initially positive. It remains so unless at some future time $v - w$ reaches zero again, when necessarily $\dot{v} - \dot{w} \leq 0$ — which is impossible, since $\dot{v} > \dot{w}$ whenever $v = w$.) But $w \to \infty$ in finite time ($\dot{w} > 0$ so that $w \to \infty$ as t increases, and as $w \to \infty$, $e^{-w}\dot{w} \approx \mu e^{-1}$, so e^{-w} reaches zero in finite time); therefore also v reaches infinity in finite time. Finally

$$v = \int_\Omega u\, d\omega \leq \sup_\Omega u, \tag{1.169}$$

since $\int_\Omega d\omega = 1$: hence $u \to \infty$ in finite time.

In fact $u \to \infty$ at isolated points, and usually at one isolated point. As blow-up is approached, one might suppose that the nature of the solution in the vicinity of the blow-up point would become independent of the initial (or boundary) conditions, and thus that some form of local similarity solution might be appropriate.

This is indeed the case, although the precise structure is rather complicated. We examine blow-up in one spatial dimension, x. As a first guess, the logarithmic nature of blow-up in the spatially independent case, together with the usual square-root behaviour of the space variable in similarity solutions for the diffusion equation, suggests that we define

$$\tau = -\ln(t_0 - t), \quad \eta = \frac{x - x_0}{(t_0 - t)^{1/2}}, \quad u = -\ln[\lambda(t_0 - t)] + g(\eta, \tau), \tag{1.170}$$

where blow-up occurs at $x = x_0$ at $t = t_0$; hence g satisfies

$$g_\tau = g_{\eta\eta} - \tfrac{1}{2}\eta g_\eta + e^g - 1. \tag{1.171}$$

The natural candidate for a similarity solution is then a steady solution $g(\eta)$ of (1.171), satisfying

$$g'' - \tfrac{1}{2}\eta g' + (e^g - 1) = 0, \tag{1.172}$$

and matching to a far field solution $u(x, t_0)$ would suggest

$$g \sim -2\ln|\eta| \quad \text{as} \quad \eta \to \pm\infty. \tag{1.173}$$

Solutions of (1.172) with this asymptotic structure do exist as either $\eta \to \infty$ or $\eta \to -\infty$ — but not at both ends simultaneously. (1.172) admits even solutions, and if we restrict ourselves to these, then we may take

$$g'(0) = 0, \quad g(0) \neq 0. \tag{1.174}$$

(If $g(0) = 0$, then $g \equiv 0$ is the solution.) However, it is found that such solutions have a different asymptotic behaviour as $\eta \to \infty$, namely

$$g \sim -\frac{A}{|\eta|} \exp\left[\tfrac{1}{4}\eta^2\right], \tag{1.175}$$

and $A = A[g(0)] > 0$ for $g(0) \neq 0$ (and $A(0) = 0$), and these cannot match to the outer solution. If one alternately prescribes (1.173) as $\eta \to +\infty$, for example, then the solution is asymmetric, and has the exponential behaviour (1.175) as $\eta \to -\infty$. Thus the appealingly simple similarity structure implied by steady solutions of (1.171) is wrong (and actually, the solution of the initial value problem (1.171) satisfying (1.173) tends to zero as $\tau \to \infty$).

However, (1.171) itself develops a local similarity structure as $\tau \to \infty$, using a further similarity variable

$$z = \frac{\eta}{\tau^{1/2}} = \frac{x - x_0}{(t_0 - t)^{1/2}[-\ln(t_0 - t)]^{1/2}}. \tag{1.176}$$

Rewriting (1.171) in terms of z and τ yields

$$g_\tau + \tfrac{1}{2} z g_z + 1 - e^g = \frac{1}{\tau}\left[g_{zz} + \tfrac{1}{2} z g_z\right]. \tag{1.177}$$

At leading order in τ^{-1} this has a solution

$$g = -\ln\left[1 + \tfrac{1}{4} c z^2\right], \tag{1.178}$$

where c is indeterminate, and this forms the basis for a formal expansion. It is algebraically convenient to use (1.178) to define c as a new variable, and also to write

$$s = \ln \tau; \tag{1.179}$$

Then (1.177) becomes

$$c_z = \frac{2}{\tau z^3}\left[2c + 4 z c_z + z^2 c_{zz} + z^2\left\{-\frac{[c + \frac{1}{2} z c_z]^2}{1 + \frac{1}{4} c z^2} + c + \tfrac{1}{2} z c_z - c_s\right\}\right]. \tag{1.180}$$

We seek a solution for (1.180) in the form

$$c \sim c_0(z, s) + \frac{1}{\tau} c_1(z, s) + \frac{1}{\tau^2} c_2(z, s)..., \tag{1.181}$$

and then, since $\tau d/d\tau = d/ds$, we have

$$c_s \sim \dot{c}_0 + \frac{1}{\tau}(\dot{c}_1 - c_1) + \frac{1}{\tau^2}(\dot{c}_2 - 2c_2) + ..., \tag{1.182}$$

where $\dot{c}_i \equiv \partial c_i / \partial s$. Substituting this into (1.180) and equating powers of τ, we find

$$c_0 = C_0(s), \tag{1.183}$$

where C_0 is arbitrary, and

$$c_{1z} = \frac{2}{z^3}\left[2C_0 + z^2\left\{-\frac{C_0^2}{1 + \frac{1}{4} C_0 z^2} + C_0 - \dot{C}_0\right\}\right]. \tag{1.184}$$

The arbitrary function C_0 arises because the order of the approximate equation is reduced. In order to specify it, and other arbitrary functions of s which arise at each order, we require that the solutions c_i be smooth, and this requires that there be no term on the right hand side of (1.184) proportional to $1/z$ as $z \to 0$, in order that logarithmic singularities not be introduced. Specifically, we require at each stage of the approximation that

$$\frac{\partial c_i}{\partial z} = \frac{2}{z^3}\left[a_{0i} + a_{1i} z + a_{3i} z^3 + \ldots\right]; \tag{1.185}$$

so that $z^2 c_i$ is smooth. Applying this to (1.184) requires that

$$\dot{C}_0 = C_0(1 - C_0), \tag{1.186}$$

so that $C_0 \to 1$ as $s \to \infty$, and then

$$c_1 = -\frac{2C_0}{z^2} + C_1(s) + C_0^2 \ln\left[1 + \tfrac{1}{4}C_0 z^2\right]. \tag{1.187}$$

At $O(1/\tau^2)$, we then have

$$\begin{aligned} c_{2z} &= \frac{2}{z^3}\left[2c_1 + 4zc_{1z} + z^2 c_{1zz} + z^2\left\{-(\dot{c}_1 - c_1) + (c_1 + \tfrac{1}{2}zc_{1z})\right.\right. \\ &\qquad \left.\left. -\frac{2c_0(c_1 + \frac{1}{2}zc_{1z})}{1 + \frac{1}{4}c_0 z^2} + \tfrac{1}{4}c_0^2 c_1 z^2(1 + \tfrac{1}{4}c_0 z^2)^2\right\}\right], \end{aligned} \tag{1.188}$$

and applying the regularity condition (1.185), we find, after some algebra,

$$\dot{C}_1 = 2(1 - C_0)C_1 + \tfrac{5}{2}C_0^3, \tag{1.189}$$

so that $C_1 \to C_{10} + \frac{5}{2}s$ as $s \to \infty$. Thus finally we obtain the local similarity solution

$$u \approx -\ln\left[\lambda\left\{t_0 - t + \frac{c(x - x_0)^2}{4[-\ln(t_0 - t)]}\right\}\right], \tag{1.190}$$

where $c \approx C_0(s)$, $s = \ln\tau = \ln[-\ln(t_0 - t)]$.

1.4.9 Reaction-diffusion equations

The development of mathematical biology in the last thirty years has led to one particular pedagogical example of wave and pattern formation, and that is in the coupled sets of equations known as reaction-diffusion equations. The general type is

$$\frac{\partial u_i}{\partial t} = f_i(\mathbf{u}) + \boldsymbol{\nabla}.[D_{ij}\boldsymbol{\nabla}u_j], \tag{1.191}$$

for n reactants $u_1, ..., u_n$, where the summation convention (sum over repeated suffixes, here j) is implied, but much of what is known about the behaviour of such systems can be illustrated with the two-species equations

$$\begin{aligned} u_t &= f(u,v) + D_1\nabla^2 u, \\ v_t &= g(u,v) + D_2\nabla^2 v. \end{aligned} \tag{1.192}$$

The phenomena which we find are closely allied to the behaviour of the underlying dynamical system

$$\begin{aligned} \dot{u} &= f(u,v), \\ \dot{v} &= g(u,v), \end{aligned} \tag{1.193}$$

and we will discuss three types of behaviour: wave trains, solitary waves, and stationary patterns.

Wave trains

One way in which periodic travelling waves, or wave trains, can arise is when the underlying kinetics described by (1.193) is oscillatory. Diffusion causes the oscillations to propagate in space, and a periodic travelling wave results. It suffices to consider components which diffuse equally rapidly, so that we may consider the suitably scaled equation

$$\mathbf{w}_t = \mathbf{f}(\mathbf{w}) + \nabla^2 \mathbf{w}, \tag{1.194}$$

where $\mathbf{w} \in \mathbf{R}^n$.

Suppose that the reaction kinetics admit an attractive limit cycle for the underlying system $\mathbf{w}_t = \mathbf{f}(\mathbf{w})$, and denote this as $\mathbf{W}_0(t)$, i.e.

$$\mathbf{W}_0' = \mathbf{f}(\mathbf{W}_0). \tag{1.195}$$

Suppose further that we look for solutions which are slowly varying in space. We define slow time and space scales τ and $\mathbf{X}$ as

$$\tau = \varepsilon t, \quad \mathbf{X} = \sqrt{\varepsilon}\mathbf{x} \tag{1.196}$$

and seek formal solutions of (1.194) in the form $\mathbf{w}(\mathbf{X}, t, \tau)$, where

$$\mathbf{w}_t + \varepsilon \mathbf{w}_\tau = \mathbf{f}(\mathbf{w}) + \varepsilon \nabla^2 \mathbf{w}, \tag{1.197}$$

and $\boldsymbol{\nabla} = \boldsymbol{\nabla}_{\mathbf{X}}$ now. Expanding $\mathbf{w}$ as

$$\mathbf{w} \sim \mathbf{w}_0 + \varepsilon \mathbf{w}_1 + \ldots \tag{1.198}$$

leads to

$$\begin{aligned} \mathbf{w}_{0t} &= \mathbf{f}(\mathbf{w}_0), \\ \mathbf{w}_{1t} - J\mathbf{w}_1 &= -\mathbf{w}_{0\tau} + \nabla^2 \mathbf{w}_0, \end{aligned} \tag{1.199}$$

and so on; here $J = D\mathbf{f}(\mathbf{w}_0)$ is the Jacobian of $\mathbf{f}$ at $\mathbf{w}_0$. After an initial transient, we may take

$$\mathbf{w}_0 = \mathbf{W}_0(t + \psi), \tag{1.200}$$

where $\psi(\tau, \mathbf{X})$ is the slowly-varying phase, and $J = D\mathbf{f}(\mathbf{W}_0)$ is a time-periodic matrix. Thus we find that $\mathbf{w}_1$ satisfies

$$\mathbf{w}_{1t} - J\mathbf{w}_1 = -(\psi_\tau - \nabla^2 \psi)\mathbf{W}_0' + |\boldsymbol{\nabla}\psi|^2 \mathbf{W}_0''. \tag{1.201}$$

Note that $\mathbf{s} = \mathbf{W}_0'$ satisfies the homogeneous equation $\mathbf{s}_t - J\mathbf{s} = \mathbf{0}$. It follows that the solution of (1.201) is

$$\mathbf{w}_1 = -t(\psi_\tau - \nabla^2 \psi)\mathbf{s} + |\boldsymbol{\nabla}\psi|^2 \mathbf{u}, \tag{1.202}$$

where

$$\mathbf{u} = M(t) \int_0^t M^{-1}(\theta) J(\theta) \mathbf{s}(\theta)\, d\theta + M(t), \tag{1.203}$$

and M is a fundamental matrix for the homogeneous equation, i. e., $M' = JM$, $M(0) = I$. Floquet's theorem implies that

$$M = Pe^{t\Lambda}, \tag{1.204}$$

where P is a periodic matrix of period T (the same as that of the limit cycle $\mathbf{W}_0$). We can take the matrix Λ to be diagonal if the characteristic multipliers are distinct, and since we assume $\mathbf{W}_0$ is attracting, the eigenvalues of Λ will all have negative real part, except one of zero corresponding to $\mathbf{s}$. With a suitable choice of basis, we then have

$$(e^{t\Lambda})_{ij} \to \delta_{i1}\delta_{j1} \quad \text{as} \quad t \to \infty, \tag{1.205}$$

i. e., a matrix with the single non-zero element being unity in the first element. In this case the first column of P is $\mathbf{s}$, i. e., $P_{i1} = s_i$.

From (1.203), we have

$$\mathbf{u} = P(t) \int_0^t e^{\eta\Lambda} P^{-1}(t-\eta) J(t-\eta) \mathbf{s}(t-\eta)\, d\eta + M\mathbf{c}. \tag{1.206}$$

The effect of the transient dies away as $t \to \infty$, and if we ignore it, then we can take $M_{ij} = s_i\delta_{j1}$, whence $M\mathbf{c} = c_1\mathbf{s}$, and thus

$$\mathbf{u} = \mathbf{s}\left[\int_0^t \alpha(\eta)\, d\eta + c_1\right], \tag{1.207}$$

where the periodic function α is given by[6]

$$\alpha = (P^{-1})_{1m} J_{mj} s_j. \tag{1.208}$$

We define the mean of α to be

$$\bar{\alpha} = \frac{1}{T}\int_0^T \alpha(\eta)\, d\eta, \tag{1.209}$$

so that

$$\beta = \int_0^t (\alpha - \bar{\alpha})\, d\eta \tag{1.210}$$

is periodic with period T. Then (1.202) is

$$\mathbf{w}_1 = [t\{-\psi_\tau + \nabla^2\psi + \bar{\alpha}|\boldsymbol{\nabla}\psi|^2\} + c_1 + \beta]\mathbf{s}, \tag{1.211}$$

and in order to suppress secular terms (those which grow in t), we require the phase ψ to satisfy the evolution equation

$$\psi_\tau = \nabla^2\psi + \bar{\alpha}|\boldsymbol{\nabla}\psi|^2. \tag{1.212}$$

This is an integrated form of Burgers' equation; in one dimension, $u = -\psi_X/2\bar{\alpha}$ satisfies $u_\tau + uu_X = u_{XX}$. Disturbances will form shocks, which are jumps of phase

[6] We use the summation convention, which implies summation over repeated suffixes.

gradient. More generally, if $\mathbf{u} = -\boldsymbol{\nabla}\psi/2\bar{\alpha}$, then (bearing in mind that $\boldsymbol{\nabla} \times \mathbf{u} = \mathbf{0}$) we find

$$\mathbf{u}_\tau + (\mathbf{u}.\boldsymbol{\nabla})\mathbf{u} = \nabla^2\mathbf{u}, \tag{1.213}$$

which is the Navier-Stokes equation with no pressure term. Phase gradients move down phase gradients, and form defects where the (sub-)characteristics intersect.[7]

Solutions of (1.212) which vary with X correspond to travelling wave trains. For example, in one dimension, waves travel locally at speed $dX/dt \approx -(\partial\psi/\partial X)^{-1}$. In general, however, the phase of the oscillation becomes constant at long times if zero flux boundary conditions $\partial\psi/\partial n = 0$ are prescribed at container boundaries, and wave trains die away. However, this takes a long time (if ε is small), and while spatial gradients are present, the solutions have the form of waves. For example, *target patterns* are created when an impurity creates a local inhomogeneity in the medium.

Suppose the effect of such an impurity is to decrease the natural oscillation period by a small amount (of $O(\varepsilon)$) near a point, which we take to be the origin. To be specific, suppose that the impurity is circular, of radius a; then it is appropriate to specify

$$\psi = \tau + c \quad \text{at} \quad R = a, \tag{1.214}$$

where R is the polar radius and c is an arbitrary constant (it merely fixes the time origin), and we expect ψ to tend towards the solution $\psi = \tau - f(R)$ as $t \to \infty$, where f satisfies

$$f'' + \frac{1}{R}f' - \bar{\alpha}f'^2 + 1 = 0, \tag{1.215}$$

together with $f(a) = c$ and an appropriate no flux condition at large R; such a condition can always be implemented by consideration of a small boundary layer near the boundary. Alternatively, we can restrict attention to a target pattern centred at the impurity by suppressing incoming waves (this is known as a radiation condition). The relevant solution if $\bar{\alpha} > 0$ is

$$f(R) = \frac{1}{\bar{\alpha}} \ln K_0(\sqrt{\bar{\alpha}}R), \tag{1.216}$$

where K_0 is the modified Bessel function of the second kind of order zero. The other Bessel function I_0 is suppressed because of the radiation condition (it produces incoming waves). At large R, $\psi \sim -R/\sqrt{\bar{\alpha}}$, which represents an outward travelling wave of speed $dR/dt \approx \sqrt{\bar{\alpha}}$. If, on the other hand, $\bar{\alpha} < 0$, then K_0 is replaced by a combination of the Bessel functions J_0 and Y_0, and the solution blows up at finite R, and travelling wave solutions of this type do not exist. More generally, if $\psi = \beta\tau$ on $R = a$, then target patterns exist if $\bar{\alpha}\beta > 0$.

[7] Physicists call (1.212) the KPZ equation (after Kardar *et al.* (1986)). The substitution $u = \exp(\bar{\alpha}\psi)$ reduces it to the diffusion equation for u; this is the Hopf–Cole transformation (see Whitham 1974).

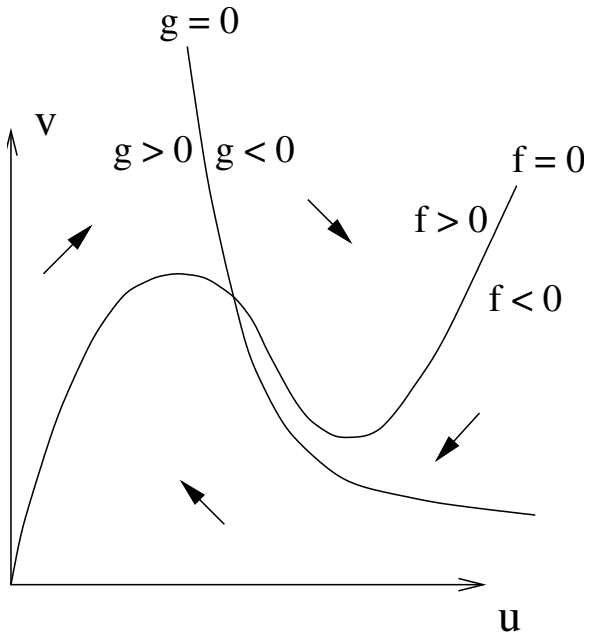

Figure 1.24: Phase diagram for kinetics of (1.217).

Activator-inhibitor system

An example of a system supporting travelling wave solutions is the activator-inhibitor system

$$\begin{aligned} u_t &= f(u,v) + \nabla^2 u, \\ v_t &= g(u,v) + \nabla^2 v, \end{aligned} \tag{1.217}$$

where the nullclines of the kinetics are as shown in figure 1.24 (cf. figure 1.6). This system is called an activator-inhibitor system because $\partial f/\partial v > 0$, thus increased v activates u, while $\partial g/\partial u < 0$, so increased u inhibits v. When the intersection is on the decreasing part of $f = 0$, as shown, then $\partial f/\partial u > 0$, $\partial g/\partial v < 0$, and $-f_u/f_v > -g_u/g_v$, whence the determinant D of the Jacobian of $(u,v)^T$ at the fixed point is positive. Hence the fixed point is unstable if $f_u + g_v > 0$, and a limit cycle exists in this case if trajectories are bounded. For example, if $f = F/\varepsilon$, $\varepsilon \ll 1$, this is the case, and the limit cycle takes the relaxational form shown in figure 1.6. The addition of diffusion allows travelling wave trains to exist, as described above.

Solitary waves in excitable media

Suppose now the intersection point of the nullclines $f = 0$ and $g = 0$ is as shown in figure 1.25. The fixed point of the underlying dynamical system is now stable, but relatively small perturbations to v can cause large excursions in u, as shown. When diffusion is included, these large excursions can travel as solitary waves. The simplest way to understand how this comes about is if we allow u to have fast reaction kinetics and take v as having zero diffusion coefficient.

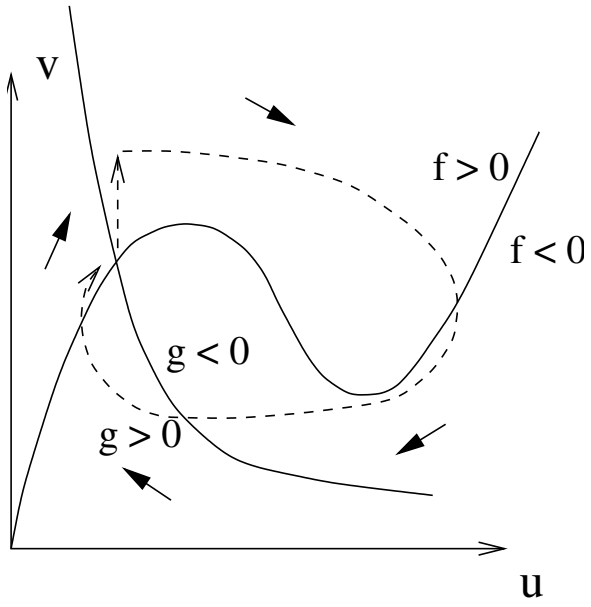

Figure 1.25: Phase plane for excitable kinetics.

In one dimension, a suitably scaled model is then

$$\begin{aligned} \varepsilon u_t &= f(u,v) + \varepsilon^2 u_{xx}, \\ v_t &= g(u,v), \end{aligned} \tag{1.218}$$

and we look for a travelling wave solution of the form

$$u = u(\xi), \quad v = v(\xi), \quad \xi = ct - x, \tag{1.219}$$

where c (assumed positive) is to be found. Then

$$\begin{aligned} \varepsilon c u' &= f + \varepsilon^2 u'', \\ c v' &= g, \end{aligned} \tag{1.220}$$

and the idea is to seek a trajectory for which $(u,v) \to (u^*, v^*)$ as $\xi \to \pm\infty$ (here (u^*, v^*) is the fixed point of the system). The form of this trajectory is shown in figure 1.26. On the slow parts of the wave, $f \approx 0$ and $cv' \approx g$. On the fast parts, we put $\xi = \varepsilon\Xi$; then $v \approx$ constant, and we denote v_+ $(= v^*)$ and v_- as the corresponding values of v; v_- is unknown (as is c).

On the fast parts of the wave, we define $u' = w$ (where now $u' = du/d\Xi$), so that

$$\begin{aligned} u' &= w, \\ w' &= cw - f_\pm(u), \end{aligned} \tag{1.221}$$

where $f_\pm(u) = f(u, v_\pm)$. The graphs of f_+ and f_- are similar, and are shown in figure 1.27, where we see that construction of the connecting branches PQ and RS requires that the fixed points P and Q, or R and S, of (1.221) have a connecting trajectory. In general, this will not be the case, but we can choose c to connect P to Q (since v_+ is known), and then we choose v_- to connect R to S (with this same value of c). The form of the resulting travelling wave is shown in figure (1.28).

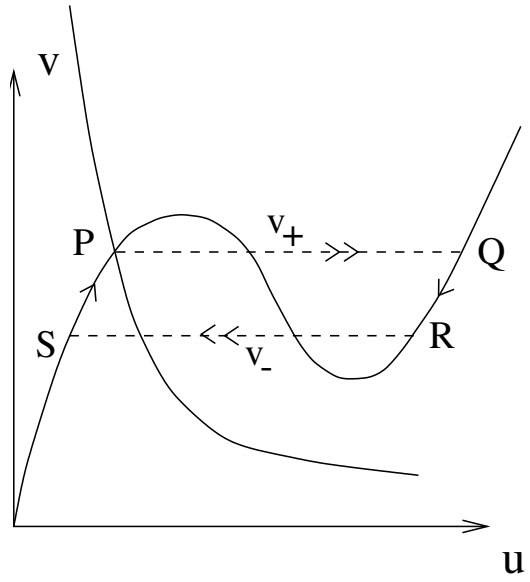

Figure 1.26: Phase plane for solitary wave trajectory.

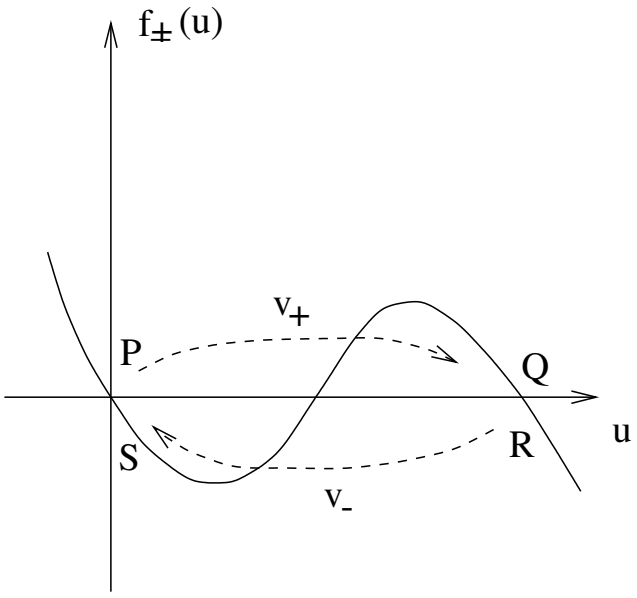

Figure 1.27: Phase plane connection for the fast parts of the travelling wave.

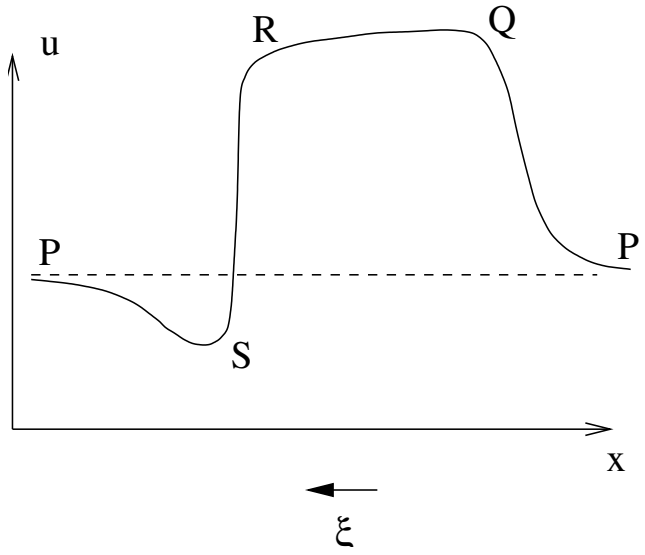

Figure 1.28: Spatial form of the travelling wave.

Pattern formation

We have seen that an activator (v)-inhibitor (u) system

$$\begin{aligned} \dot{u} &= f(u,v), \\ \dot{v} &= g(u,v), \end{aligned} \tag{1.222}$$

admits periodic travelling waves when the uniform state is unstable, and solitary waves when it is stable (and the activator diffuses slowly). Stationary patterns can occur when a stable steady state of (1.222) is rendered spatially unstable by different component diffusivities. Suppose that

$$\begin{aligned} u_t &= f(u,v) + u_{xx}, \\ v_t &= g(u,v) + dv_{xx}, \end{aligned} \tag{1.223}$$

is an activator-inhibitor system with $f_v > 0$, $g_u < 0$; the restriction to one spatial dimension is inconsequential. The parameter d here represents the ratio of activator to inhibitor diffusivities. Note that when $d \to 0$, we expect solitary wave propagation, at least for the phase diagram of figure 1.25, where also $f_u < 0$, $g_v < 0$ at the fixed point.

With the stationary state denoted as (u^*, v^*), we assume it is stable in the absence of diffusion; thus assume

$$\begin{aligned} T &= f_u + g_v < 0, \\ \Delta &= f_u g_v - f_v g_u > 0, \end{aligned} \tag{1.224}$$

both evaluated at (u^*, v^*). We put

$$\begin{pmatrix} u \\ v \end{pmatrix} = \begin{pmatrix} u^* \\ v^* \end{pmatrix} + \mathbf{w} e^{\sigma t + ikx}; \tag{1.225}$$

linearisation of (1.223) then yields

$$(M - k^2 D - \sigma)\mathbf{w} = \mathbf{0}, \tag{1.226}$$

where

$$M = \begin{pmatrix} f_u & f_v \\ g_u & g_v \end{pmatrix}, \quad D = \begin{pmatrix} 1 & 0 \\ 0 & d \end{pmatrix}. \tag{1.227}$$

The eigenvalues σ are the roots of

$$\sigma^2 - T_d\sigma + \Delta_d = 0, \tag{1.228}$$

where

$$\begin{aligned} T_d &= T - (1+d)k^2, \\ \Delta_d &= \Delta - k^2(df_u + g_v) + dk^4. \end{aligned} \tag{1.229}$$

The steady state is stable if and only if $T_d < 0$ and $\Delta_d > 0$ (cf. figure 1.4). Now $T < 0$ and $\Delta > 0$ by assumption: hence $T_d < 0$, and thus instability occurs if and only if $\Delta_d < 0$. Since $\Delta > 0$, we see from (1.227) that this can only occur if $df_u + g_v > 0$. Thus either $f_u > 0$ or $g_v > 0$, and the system cannot be excitable. Since $f_u + g_v < 0$, we see that a necessary condition for instability is that $d \neq 1$. Because d is the ratio of two diffusivities, this instability is known as *diffusion-driven instability* (DDI), or *Turing instability*, after the originator of the theory.

To be specific, let us suppose the situation to be that of figure 1.24, i. e., $f_u > 0$, $g_v < 0$: then we require $d > 1$ for DDI. The precise criterion for instability is that $\min \Delta_d < 0$, and, from (1.229), this is

$$df_u + g_v > 2[\Delta d]^{1/2}, \tag{1.230}$$

and this can be reduced to

$$d > \left[\frac{\Delta^{1/2} + \{f_v|g_u|\}^{1/2}}{f_u}\right]^2. \tag{1.231}$$

The resulting instability is direct and not oscillatory (in time), though it is oscillatory in space. We can therefore expect stationary finite amplitude patterns to emerge as the stable solutions, and this is indeed what often occurs.

The form of these putative steady solutions as d becomes large can be studied by seeking (spatially) periodic solutions of

$$\begin{aligned} u_{xx} + f(u,v) &= 0, \\ v_{xx} + \varepsilon^2 g(u,v) &= 0, \end{aligned} \tag{1.232}$$

where we define $\varepsilon^2 = 1/d \ll 1$.

We begin by seeking solutions with period of $O(1)$. As u varies over distances of $x = O(1)$, $v = \bar{v}$ is approximately constant, and thus the equation for u can be integrated to give the first integral

$$\tfrac{1}{2}u_x^2 + V(u,\bar{v}) = E, \tag{1.233}$$

where

$$V(u,v) = \int_0^u f(u,v)\,du, \tag{1.234}$$

and E is constant.

The forms of the curves $f(u,v) = 0$ (defining v as a function of u), $f(u,v)$ as a function of u for various fixed v, and $V(u,v)$ as a function of u are shown in figure 1.29. For constant v, solutions for u will be periodic if they lie in the potential well of V. Given $\bar{v}$ and E, these periodic solutions are fully determined, and in particular their period P is a function of $\bar{v}$ and E, thus $P = P(\bar{v}, E)$. The choice of $\bar{v}$ and E must then be made so that v is periodic. We can choose the origin of x so that u is maximum there; then in fact u is even, and hence so is $g[u(x;\bar{v},E),\bar{v}]$. Integration of $(1.232)_2$ then yields

$$v = \bar{v} - \varepsilon^2 \int_{-P/2}^{x} (x-\xi) g[u(\xi;\bar{v},E),\bar{v}]\,d\xi, \tag{1.235}$$

where periodicity of v requires that

$$\int_{-P/2}^{P/2} g[u(\xi;\bar{v},E),\bar{v}]\,d\xi = 0. \tag{1.236}$$

(We also require that

$$\int_{-P/2}^{P/2} \xi g[u(\xi;\bar{v},E),\bar{v}]\,d\xi = 0, \tag{1.237}$$

but this is satisfied automatically since the integrand is odd.)

Given $\bar{v}$, (1.236) appears to determine E, and thus provide a one-parameter family of periodic solutions. However, it is unlikely that (1.236) can generally be satisfied for a given function g. Consideration of figure 1.29 suggests that it is more likely that, given $\bar{v}$ and E, satisfaction of (1.236) will depend on the precise location of the curve $g = 0$. For a function $g(u,v;\alpha)$ dependent on a single parameter α, such as $g = \alpha - u^3 v$, this suggests that (1.236) may be satisfied (if at all) for a unique value of $\alpha(\bar{v},E)$. Since also $P = P(\bar{v},E)$, this suggests a one-parameter family of spatially periodic solutions in which $P = P(\alpha)$.

The other possibility for periodic solutions involves the existence of regions in which u is constant, separated by boundary layers in which u changes rapidly. In this case, the longer space scale $X = \varepsilon x$ comes into play, and the resultant form of the equations (1.232),

$$\begin{aligned} \varepsilon^2 u_{XX} + f &= 0, \\ v_{XX} + g &= 0, \end{aligned} \tag{1.238}$$

is clearly suggestive of a boundary layer structure.

The boundary layers themselves are still described by (1.233), but now we require that u tends to constants $\bar{u}_+$ and $\bar{u}_-$ as $x \to \pm\infty$; this requires $\bar{v}$ to have the particular value where the local maxima of $V(u,\bar{v})$ are the same (and these occur at $\bar{u}_-$ and $\bar{u}_+$).

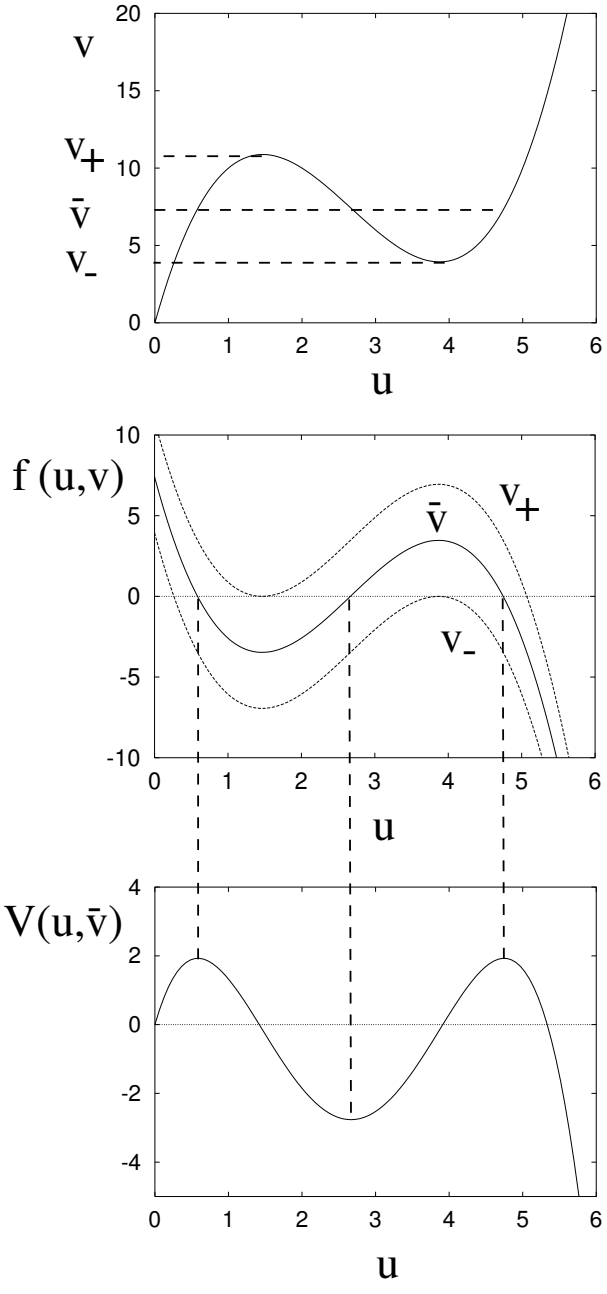

Figure 1.29: Definition of the values $v_\pm$ defined by the function $f(u,v)$. The upper graph shows the curve defined implicitly by $f(u,v)=0$ (compare figure 1.24). The middle graph shows the function $f(u,v)$ as a function of u for $v = v_+, \bar{v}, v_-$, and the lowest graph is the potential $V(u,v) = \int_0^u f(u,v)\,du$ for the value of $v=\bar{v}$ corresponding to the middle of these three curves. The choice of $\bar{v}$ in the figure is that for which the two maxima of V are equal. The particular function used in the illustrations is $f(u,v) = v-[u^3-8u^2+17u]$, for which the value of $\bar{v}$ where the maxima are equal is $\bar{v}\approx 7.407$; the values of v_+ and v_- are $v_+\approx 10.879$ and $v_-\approx 3.935$.

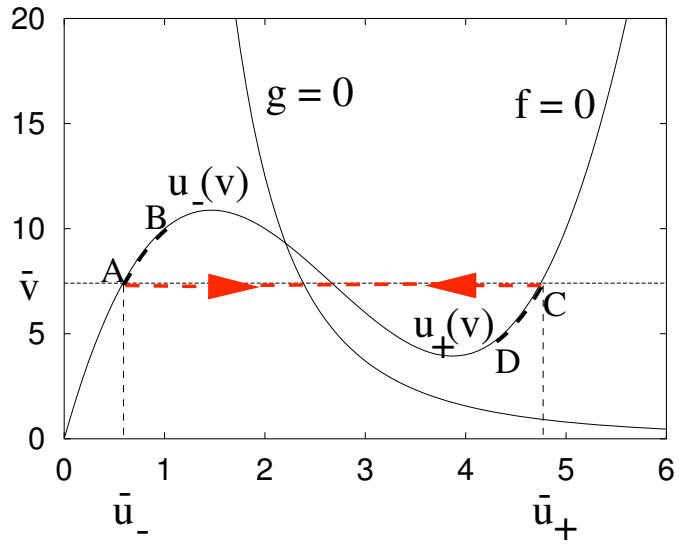

Figure 1.30: The nullclines $f(u,v)=0$ and $g(u,v)=0$. The f nullcline defines locally two functions $u_\pm(v)$. During the oscillation, v moves from A to B and back to A, while $g>0$, and similarly from C to D and back to C while $g>0$. When v reaches $\bar{v}$, a boundary layer in u switches the solution between its two branches.

For the value of E equal to this maximum, there are then boundary layer solutions in which either u goes from $\bar{u}_-$ to $\bar{u}_+$ as x increases, or from $\bar{u}_+$ to $\bar{u}_-$.

The periodic solutions are filled out by solving

$$v_{XX} + g(u,v) = 0, \tag{1.239}$$

in which u is determined by $f(u,v)=0$. There are two branches of the resultant function $u(v)$, which we denote by $u_-(v)$ and $u_+(v)$ (and $u_\pm(\bar{v})=\bar{u}_\pm$), as indicated in figure 1.30; if we define

$$W(v) = \begin{cases} \displaystyle\int_{\bar{v}}^{v} g\left[u_-(v'),v'\right]\,dv' & \text{for} \quad \bar{v} < v, v_+, \\ \displaystyle\int_{\bar{v}}^{v} g\left[u_+(v'),v'\right]\,dv' & \text{for} \quad v_- < v < \bar{v}, \end{cases} \tag{1.240}$$

then W is a V-shaped function defined in $[v_-,v_+]$, with a minimum at $v=\bar{v}$. Solutions for v are determined from

$$\tfrac{1}{2}v_X^2 + W(v) = F, \tag{1.241}$$

for constant F, and determine a one-parameter family of periodic solutions. Note that this family occurs for a fixed choice of f and g, and the parameter can be taken to be the period. This family is then naturally interpreted as the continuation to large d of the bifurcating family dependent on wave number which arises when (1.231) is satisfied.

1.5 Notes and references

Modelling

By mathematical modelling, I mean the formulation of a problem in mathematical terms. If the process is continuous, usually the model will take the form of differential equations, and in this book we further confine ourselves to deterministic models, as opposed to stochastic models. Stochastic models are of increasing popularity, aiming as they do to represent the noisiness of a system, but they can also be something of an excuse to sweep things we don't understand under the carpet.

The original classic book which set out the applied mathematician's stall is that by Lin and Segel (1974). It contains the ethos of applied mathematics, but retained a somewhat austere choice of applications. Another classic book which dealt much more with practical (mostly industrial) applications is that by Tayler (1986). My own book (Fowler 1997) is in a similar spirit.

These books, certainly the latter two, are aimed at graduate level. There are a number of books which deal more gently, but still genuinely, with modelling. The classic of this type is perhaps that by Haberman (1998), a reprinted edition of his 1977 text. More recent books in this direction are those by Fowkes and Mahony (1994), Howison (2005), and Holmes (2009).

Asymptotics and perturbation theory

Like modelling, there are many books on perturbation methods. To my mind, the pre-eminent ones are those by Kevorkian and Cole (1981), Bender and Orszag (1978) and Hinch (1991). Van Dyke's (1975) book is also a classic. Other well known books are those by Nayfeh (1973) and Holmes (1995).

The flavours of these books are subtly different. Bender and Orszag's blockbuster, taught at M. I. T. in a one-semester course (the whole book), has as its central part the asymptotic study of boundary layers. The book has the novelty of giving many numerical illustrations of how good (or bad) the approximations are, and when they appear to break down.

Kevorkian and Cole's book (an expanded edition of Cole's original 1968 monograph) focusses more on multiple scale methods, and takes these to levels of sophistication a good deal beyond more elementary texts, and there are expositions of some classic problems: the derivation of the Korteweg-de Vries equation describing long waves in shallow water, and the relaxational van der Pol oscillator, for example.

Van Dyke's book is slightly more formal in nature, and mostly concerned with fluid mechanics. It is one of the few places where one can learn the method of strained coordinates, a method which is particularly useful in dealing with the motion of margins and fronts. Hinch's and Nayfeh's books include a chapter on strained coordinates also, as well as the other staple contents. Hinch's is short, to the point, succinct. Holmes's book includes a chapter on homogenisation.

Combustion, nonlinear diffusion and blow-up

Two early accounts of combustion and exothermic reactions are those by Aris (1975) and Buckmaster and Ludford (1982). The first of these largely deals with reaction in (solid) permeable catalysts, while combustion theory of the second tends to deal with gaseous combustion, where the theory has all the complication of compressible gas dynamics together with the species reaction kinetics. A more mathematical book is that by Bebernes and Eberly (1989). Other books on this subject include those of Williams (1985), Barnard and Bradley (1985) and Glassman (1987), the latter two more descriptive than Williams's voluminous work. A similar analytic approach is that by Liñán and Williams (1993), but this book is more concise than that of Williams. Combustion really applies to any reaction, but by convention refers specifically to reactions where there is a large change of temperature. If this is such that the reactants become luminous, we have a flame. If the change of temperature is rapid, we have a thermal explosion. Since in gases, increase of temperature is associated with increase of pressure, explosions tend to be associated with shock waves, or detonation waves, and this is the explosive 'blast'.

The classical treatment of thermal explosions (in solids) is much as described in section 1.4.8, and involves the positive feedback associated with exothermic reactive heating, which causes the runaway. Explosive runaway can also be caused by autocatalytic feedback in the reaction scheme, much as in a nuclear explosion; this is the 'chain' reaction. Systems with autocatalysis are also prone to oscillatory bifurcations and waves, and are dealt with in the book by Gray and Scott (1990). Ignition of explosions may be caused by impact or friction (as in striking a match). Both events cause a localised hotspot to occur, that of impact being due to the sudden compression of small gas bubbles, see Bowden and Yoffe (1985).

Reactions in a diffusive flame (i. e., one where fuel and oxidant are not pre-mixed) can be analysed using large activation energy asymptotics; the reactions occur in a narrow front which spreads as a deflagration wave, whose speed is less than the sound speed, and is rate-limited by the supply of reactant to the front. The detonation wave is a reactive shock wave, in which the reaction is triggered not by supply of reactant, but by gas compression and consequent heating within the shock.

The book by Samarskii *et al.* (1995) provides a wealth of information about nonlinear diffusion equations, and their associated solution properties of compact support and blow up. The asymptotic description given here of the local similarity structure for the blow up of solutions of $u_t = u_{xx} + \lambda e^u$ is based on that of Dold (1985).

Burgers' equation

Burgers' equation relates to a model introduced by Burgers (1948) to describe turbulence in fluid flow in a pipe. In its original form, his model is given by the pair of

equations

$$\begin{aligned} b\frac{dU}{dt} &= P - \frac{\nu U}{b} - \frac{1}{b}\int_0^b v^2\,dy, \\ \frac{\partial v}{\partial t} + 2v\frac{\partial v}{\partial y} &= \frac{Uv}{b} + \nu\frac{\partial^2 u}{\partial y^2}. \end{aligned} \tag{1.242}$$

This is a toy model which aims to mimic the classical procedure of Reynolds averaging, leading to an evolution equation for the mean flow $U(t)$, and another for the fluctuating velocity field $v(y,t)$. The cross stream variable is y, and the width of the 'pipe' is b. Burgers' equation follows from the assumption that $U = 0$, and arises in the original paper as an approximation to describe the transition region near shocks; Burgers gives the travelling wave front solution for this case. A thprough discussion of Burgers' equation is given by Whitham (1974).

Fisher's equation

The geneticist R. A. Fisher wrote down his famous equation (Fisher 1937) to describe the propagation of an advantageous gene in a population situated in a one dimensional continuum — Fisher had in mind a shore line as an example. The genes (or more properly *alleles*, i. e., variants of genes), reside in the members of a population, and the proportion of different alleles of any particular gene is described by Hardy–Weinberg kinetics. If one allele has a slight evolutionary advantage, then its proportion p will vary slowly from generation to generation, and its rate of change is given in certain circumstances by the logistic equation $\dot{p} = kp(1-p)$. The effect of diffusion allows the genes to migrate through the migration of the carrier population. See Hoppensteadt (1975) for a succinct description. Fisher did not bother with all this background, but simply wrote his equation down directly. As well as this paper, he authored or co-authored eight other papers in the same volume, as well as being the journal editor!

Solitons

There are many books on solitons. An accessible introduction is the book by Drazin and Johnson (1989), and a more advanced treatment is that of Newell (1985). The subject is rich and fascinating, as is also the curious discovery of the 'first' soliton, or 'great wave of translation' by John Scott Russell in 1834, as he followed it on horseback along the Edinburgh to Glasgow canal. The Korteweg–de Vries equation which appears successfully to describe such waves was introduced by them much later (Korteweg and de Vries 1895), by which time they are referred to as solitary waves. Korteweg and de Vries also wrote down the periodic (but unstable) *cnoidal* wave solutions.

There are many other equations which are now known to possess soliton solutions, and their folklore has crept into many subjects. Under the guise of 'magmons', for example, they have appeared in the subject of magma transport, which we discuss in chapter 9.

Reaction–diffusion equations

Any book on mathematical biology (and there are a good number of these) will discuss reaction–diffusion equations. The gold standard of the type is the book (now in two volumes) by Murray (2002), which also contains much other subject matter. A more concise book just on reaction–diffusion equations is that by Grindrod (1991). These books span the undergraduate/graduate transition. The book by Edelstein-Keshet (2005) is gentler, and aimed at a lower level.

Kopell and Howard (1973) and Howard and Kopell (1977) studied waves in reaction-diffusion equations using the ideas of bifurcation theory and multiple scales. Keener (1980, 1986) studied spiral wave formation in excitable media, using as a template a singularly perturbed pair of equations, essentially of Fitzhugh–Nagumo type.

Meinhardt (1982) studied pattern formation in reaction-diffusion systems, and later (Meinhardt 1995) studied the relation between a suite of mathematical models and actual observed patterns on sea shells. The comparison is striking as well as pictorially sumptuous.

Exercises

1.1 Suppose

$$Pe\left[\frac{\partial T}{\partial t}+\mathbf{u}.\boldsymbol{\nabla}T\right]=\nabla^2 T+1 \ \text{ in } \ D,$$

with

$$\begin{aligned} T &= 0 \ \text{ on } \ \partial D, \\ T &= \Lambda\Theta(\mathbf{x}) \ \text{ in } \ D \ \text{ at } \ t=0, \end{aligned}$$

and $\Theta = O(1)$, $\Lambda \gg 1$, $Pe \ll 1$. Discuss appropriate scales for the various phases of the solution.

1.2 The differential equation

$$\dot{x} = a - xe^{-x}, \quad x > 0, \quad a > 0,$$

may have $0, 1$ or 2 steady states. Determine how these depend on a, and describe how solutions behave for $a > e^{-1}$ and $a < e^{-1}$, depending on the value of $x(0)$.

1.3 Each of the equations

$$\begin{aligned} z^5 - \varepsilon z - 1 &= 0, \\ \varepsilon z^5 - z - 1 &= 0, \end{aligned}$$

has five (possibly complex) roots. Find leading order approximations to these if $\varepsilon \ll 1$. Can you refine the approximations?

1.4 u and v satisfy the ordinary differential equations

$$\begin{aligned} \dot{u} &= k_1 - k_2 u + k_3 u^2 v, \\ \dot{v} &= k_4 - k_3 u^2 v, \end{aligned}$$

where $k_i > 0$. By suitably scaling the equations, show that these can be written in the dimensionless form

$$\begin{aligned} \dot{u} &= a - u + u^2 v, \\ \dot{v} &= b - u^2 v, \end{aligned}$$

where a and b should be defined. Show that if u, v are initially positive, they remain so. Draw the nullclines in the positive quadrant, show that there is a unique steady state and examine its stability. Are periodic solutions likely to exist?

1.5 The relaxational form of the van der Pol oscillator is

$$\varepsilon \ddot{x} + (x^2 - 1)\dot{x} + x = 0, \quad \varepsilon \ll 1.$$

A suitable phase plane is spanned by (x, y), where $y = \varepsilon \dot{x} + \frac{1}{3}x^3 - x$. Describe the motion in this phase plane, and find, approximately, the period of the relaxation oscillation. What happens if $\varepsilon < 0$?

1.6 Find a scaling of the combustion equation

$$c\frac{dT}{dt} = -k(T - T_0) + A \exp\left(-\frac{E}{RT}\right),$$

so that it can be written in the form

$$\dot{\theta} = \theta_0 - g(\theta),$$

where $\theta_0 = RT_0/E$ and $g = \theta - \alpha e^{-1/\theta}$. Give the definition of α. Hence show that the steady state θ is a multiple-valued function of θ_0 if $\alpha > \frac{1}{4}e^2$.

Find approximations to the smaller and larger positive roots of $x^2 e^{-x} = \varepsilon$, where ε is small and positive. Hence find the approximate range (θ_-, θ_+) of θ_0 for which there are three steady solutions.

Suppose that $\alpha > \frac{1}{4}e^2$, and θ_0 varies slowly according to

$$\dot{\theta}_0 = \varepsilon(\theta^* - \theta),$$

where $\varepsilon \ll 1$. Show that there are three possible outcomes, depending on the value of θ^*, and describe them.

1.7 A forced pendulum is modelled by the (dimensional) equation

$$l\ddot{\theta} + k\dot{\theta} + g \sin\theta = \alpha \sin \lambda t.$$

By non-dimensionalising the equation, show how to obtain (1.47), and identify the parameters $\varepsilon, \beta, \Omega_0$ and ω.

1.8 It is asserted after (1.59) that $\Omega(A)$ is a decreasing function of A for $0 < A < \pi$, or equivalently, that the function

$$p(A) = \frac{1}{\sqrt{2}} \int_0^A \frac{du}{[\cos u - \cos A]^{1/2}}$$

is increasing. Show that this is true by writing p in the form

$$p = \int_0^1 \left(\frac{\theta}{\sin\theta}\right)^{1/2} \left(\frac{\phi}{\sin\phi}\right)^{1/2} \frac{dw}{(1-w^2)^{1/2}}$$

for some functions $\theta(w, A)$ and $\phi(w, A)$, and using the fact that $\theta/\sin\theta$ is an increasing function of θ in $(0, \pi)$.

[Hint: $\cos u - \cos A = 2\sin\left(\frac{A-u}{2}\right)\sin\left(\frac{A+u}{2}\right)$.]

1.9 A simple model for the two-phase flow of two fluids along a tube is

$$\alpha_t + (\alpha v)_z = 0$$

$$-\alpha_t + [(1-\alpha)u]_z = 0$$

$$\rho_g[(\alpha v)_t + (\alpha v^2)_z] = -\alpha p_z,$$

$$\rho_l[\{(1-\alpha)u\}_t + \{D_l(1-\alpha)u^2\}_z] = -(1-\alpha)p_z,$$

where p is pressure, u and v are the two fluid velocities, α is the volume fraction of the fluid with speed v, ρ_g is its density, and ρ_l is the density of the other fluid. Show that there are two characteristic speeds $dz/dt = \lambda$, satisfying

$$(\lambda - u)^2 = (D_l - 1)[u^2 + 2u(\lambda - u)] - s^2(\lambda - v)^2,$$

where

$$s = \left[\frac{\rho_g(1-\alpha)}{\rho_l \alpha}\right]^{1/2}.$$

Deduce that the characteristic speeds are real if, when $D_l - 1 \ll 1$, $s \ll 1$,

$$D_l \gtrsim 1 + \left\{\frac{s(u-v)}{u}\right\}^2.$$

In particular, show that the roots are complex if $D_l = 1$ and $u \neq v$. What does this suggest concerning the well-posedness of the model?

1.10 The function $u(x, t)$ satisfies

$$u_t + uu_x = \alpha(1 - u^2)$$

for $-\infty < x < \infty$, with $u = u_0(x)$ at $t = 0$, and $0 < u_0 < 1$ everywhere. Show that the characteristic solution can be written parametrically in the form

$$u = \frac{u_0(s) + \tanh\alpha t}{1 + u_0(s)\tanh\alpha t}, \qquad \exp[\alpha(x-s)] = \frac{\operatorname{sech}\alpha t}{1 - u\tanh\alpha t}.$$

Sketch the form of the characteristics for an initial function such as $u_0(s) = a/(1+s^2)$. Show that, in terms of s and t, u_x is given by

$$u_x = \frac{[\alpha \operatorname{sech}^2 \alpha t] u_0'(s)}{[1 + u_0(s) \tanh \alpha t][\alpha + \{u_0'(s) + \alpha u_0(s)\} \tanh \alpha t]},$$

and deduce that a shock will form if $u_0' + \alpha(1+u_0)$ becomes negative for some s. Show that if $u_0 = a/(1+s^2)$ and a is small, this occurs if

$$\alpha \lesssim \frac{3a\sqrt{3}}{8}.$$

1.11 Discuss the formation of shocks and the resulting shock structure for the equation

$$u_t + u^\alpha u_x = \varepsilon [u^\beta u_x]_x,$$

where $\alpha, \beta > 0$, and $\varepsilon \ll 1$. (Assume $u > 0$, and $u \to 0$ at $\pm\infty$.)

Show that the equation

$$u_t + u u_x = \varepsilon u u_{xx}$$

admits a shock structure when $\varepsilon \ll 1$, but that the shock speed is *not* given by $\dot{x}_S = \frac{1}{2}(u_+ + u_-)$ (cf. (1.74)). Why should this be so?

1.12 Use phase plane methods to study the existence of travelling wave solutions to the equation

$$u_t = u^p(1 - u^q) + [u^r u_x]_x,$$

when (i) $p = 1$, $q = 2$, $r = 0$; (ii) $p = 1$, $q = 1$, $r = 1$.

1.13 Two examples of integrable partial differential equations which admit soliton solutions are the nonlinear Schrödinger (NLS) equation

$$i u_t = |u|^2 u + u_{xx},$$

and the sine-Gordon equation

$$u_{tt} - u_{xx} = \sin u.$$

Show that these equations admit solitary wave solutions (which are in fact solitons).

1.14 Write down the equation satisfied by a similarity solution of the form $u = t^\beta f(\eta)$, $\eta = x/t^\alpha$, for the equation

$$u_t = (u^m u_x)_x \quad \text{in} \quad 0 < x < \infty,$$

where $m > 0$, with $u^m u_x = -1$ at $x = 0$, $u \to 0$ as $x \to \infty$, $u = 0$ at $t = 0$. Show that $\displaystyle\int_0^\infty f \, d\eta = 1$, and hence show that in fact f reaches zero at a finite value η_0. Is the requirement that $m > 0$ necessary?

1.15 u satisfies the equation

$$u_t = [D(u)u_x]_x \quad \text{in} \quad 0 < x < \infty,$$

with $u = 0$ at $x \to \infty$ and $t = 0$. For a general function D (not a power of u), for what kind of boundary condition at $x = 0$ does a similarity solution exist? What if, instead, $D = D(u_x)$? Write down suitable equations and boundary conditions for the similarity function in each case.

1.16 The depth of a small droplet, h, satisfies the surface-tension controlled equation

$$h_t = -\frac{\gamma}{3\mu}\boldsymbol{\nabla}.[h^3\boldsymbol{\nabla}\nabla^2 h].$$

Suppose that a small quantity $\int h\,dA = M$ is released at time zero at the origin. Find a suitable similarity solution in one and two horizontal spatial dimensions.

1.17 A gravity-driven droplet of fluid spreads out on a flat surface. Its viscosity μ is a function of shear rate, so that a lubrication approximation leads to the model for its depth h, shear stress $\boldsymbol{\tau}$ and velocity $\mathbf{u}$:

$$\rho g\boldsymbol{\nabla} h = \frac{\partial \boldsymbol{\tau}}{\partial z},$$

$$\frac{\partial \mathbf{u}}{\partial z} = A|\tau|^{n-1}\boldsymbol{\tau}.$$

(A constant viscosity fluid has $n = 1$.) Show that the horizontal fluid flux is

$$\mathbf{q} = -\frac{A(\rho g)^n}{n+2}|\boldsymbol{\nabla} h|^{n-1}h^{n+2}\boldsymbol{\nabla} h,$$

and deduce that

$$\frac{\partial h}{\partial t} = \frac{A(\rho g)^n}{n+2}\boldsymbol{\nabla}.[h^{n+2}|\boldsymbol{\nabla} h|^{n-1}\boldsymbol{\nabla} h].$$

Non-dimensionalise the model, assuming initial emplacement of a finite volume M at the origin, and find similarity solutions in one and two dimensions for the depth. What happens as $n \to \infty$ or $n \to 0$?

1.18 The depth h of a symmetric (two-dimensional) droplet under the influence of gravity and surface tension is described by the dimensionless equation

$$\frac{\partial h}{\partial t} = \frac{\partial}{\partial x}\left[h^3\frac{\partial}{\partial x}\left\{Bh - \frac{\partial^2 h}{\partial x^2}\right\}\right],$$

subject to the conditions

$$h = 0,\ h_x = \mp\tan\theta \quad \text{at} \quad x = \pm x_0, \qquad \int_{-x_0}^{x_0} h\,dx = A,$$

where θ is the contact angle. Show that there is a steady state solution $h = h_0 u(x)$, in which

$$\int_u^1 \frac{du}{[(1-u)(\rho-u)]^{1/2}} = \sqrt{B}|x|,$$

the coefficient ρ is defined by

$$\rho = \frac{\tan^2\theta}{Bh_0^2},$$

and the maximum depth h_0 is given by

$$\frac{A\sqrt{B}}{2h_0} = I(\rho),$$

where

$$I(\rho) = \int_0^1 \frac{u\,du}{[(1-u)(\rho-u)]^{1/2}}.$$

By considering (graphically) both sides of the equation for h_0 as functions of ρ, show that there is a unique value of h_0 satisfying this equation, and thus a unique solution for h.

By evaluating the integrals explicitly, show that

$$u = 1 - (\rho-1)\sinh^2\left(\frac{\sqrt{B}x}{2}\right),$$

and that ρ is determined by

$$\frac{AB}{2\tan\theta} = -1 + \frac{\rho+1}{2\sqrt{\rho}}\ln\left(\frac{\sqrt{\rho}+1}{\sqrt{\rho}-1}\right).$$

Find explicit approximations for h when $AB \gg \tan\theta$ and $AB \ll \tan\theta$, and hence show that the margin positions are approximately given by

$$x_0 = \begin{cases} \dfrac{A\sqrt{B}}{\tan\theta}, & AB \gg \tan\theta, \\ \left(\dfrac{3A}{2\tan\theta}\right)^{1/2}, & AB \ll \tan\theta. \end{cases}$$

[*Note that if θ is the actual contact angle, then implicitly, the depth scale and lateral length scale have been taken equal, and the derivation of the equation for h via lubrication theory is only self consistent if $h_0 \ll 1$ or $x_0 \gg 1$. Since a length scale can be prescribed from the initial droplet size, we can choose $A = 1$ without loss of generality. We can then find conditions on B and $\tan\theta$ which ensure self consistency.*]

1.19 Let u satisfy

$$u_t = \lambda u^p + u_{xx},$$

with $u = 1$ on $x = \pm 1$ and $t = 0$. Prove that if λ is large enough, u must blow up in finite time if $p > 1$. Supposing this happens at time t_0 at $x = 0$, show that a possible local similarity structure is of the form

$$u = \frac{f(\xi)}{(t_0 - t)^\beta}, \quad \xi = \frac{x}{(t_0 - t)^{1/2}},$$

and prove that $\beta = 1/(p-1)$. Show that in this case, f would satisfy

$$f'' - \tfrac{1}{2}\xi f' + \lambda f^p - \beta f = 0,$$

and explain why appropriate boundary conditions would be

$$f \sim |\xi|^{-2\beta} \quad \text{as} \quad \xi \to \pm\infty,$$

and show that such solutions might be possible. Are any other limiting behaviours possible?

1.20 When an oscillatory reaction-diffusion system has an imperfection of size comparable to, or larger than, the wave length, then spiral waves can occur. This is because the wave trains need not be in phase round the boundary of the obstacles. For example, consider a slowly varying system (1.194) with solutions $\mathbf{w} \approx \mathbf{W}_0(t + \psi)$, where ψ satisfies the equation

$$\psi_\tau = \nabla^2 \psi + \bar{\alpha} |\boldsymbol{\nabla} \psi|^2.$$

Suppose that the imperfection is of radius a, and that the effect of the surface is to alter the period, so that we take $\psi = \beta\tau + m\theta + c$ on $r = a$, where m is an integer (so that $\mathbf{w}$ is single valued, if we suppose the period of $\mathbf{W}_0$ is normalised to be 2π); c is an arbitrary constant, which we can choose for convenience.

Put $\psi = \beta\tau + m\theta - \phi(r)$, and show that ϕ satisfies the equation

$$\phi'' + \frac{1}{r}\phi' - \bar{\alpha}\left[\phi'^2 + \frac{m^2}{r^2}\right] + \beta = 0.$$

Hence show that

$$\phi = -\frac{1}{\bar{\alpha}} \ln w(\lambda r),$$

where $w(z)$ satisfies Bessel's equation in the form

$$w'' + \frac{1}{z} w' + \left[s - \frac{\nu^2}{z^2}\right] w = 0, \qquad (*)$$

providing we choose

$$\lambda = |\bar{\alpha}\beta|^{1/2}, \quad \nu = i|\bar{\alpha} m|, \quad s = -\operatorname{sgn}(\bar{\alpha}\beta).$$

The solutions of $(*)$ when $s = 1$, i. e., $\bar{\alpha}\beta < 0$, are the Hankel functions

$$H_\nu^{(1,2)}(z) = J_\nu(z) \pm iY_\nu(z) \sim \left(\frac{2}{\pi z}\right)^{1/2} \exp\left[\pm i\left(z - \tfrac{1}{2}\nu\pi - \tfrac{1}{4}\pi\right)\right]$$

as $z \to \infty$. If $\bar{\alpha}\beta > 0$, so that $s = -1$, then the solutions are the modifed Bessel functions $I_\nu(z)$ and $K_\nu(z)$, and we have

$$I_\nu \sim \frac{1}{\sqrt{2\pi z}} e^z, \quad K_\nu \sim \left(\frac{\pi}{2z}\right)^{1/2} e^{-z}$$

as $z \to \infty$.[8]

Deduce that solutions of this type exist if $\bar{\alpha}\beta > 0$, and that in this case the presumption of outward travelling waves (the radiation condition) requires us to choose $w = K_\nu(z)$. Show that as $r \to \infty$ in this case,

$$\mathbf{w} \approx \mathbf{W}_0 \left[t + \beta\tau + m\theta - \left(\frac{\beta}{\bar{\alpha}}\right)^{1/2} r + O(\ln r) \right].$$

This solution represents a spiral wave. Note that the integer m is unconstrained. Its specification would require a model for the reaction on the surface of the impurity at $r = a$. It is plausible to imagine that such angle dependent phases arise through bifurcation of the surface reaction model as the impurity size increases.

1.21 The Fitzhugh-Nagumo equations are

$$\begin{aligned} \varepsilon u_t &= u(a-u)(u-1) - v + \varepsilon^2 u_{xx}, \\ v_t &= bu - v, \end{aligned}$$

where $0 < a < 1$, $\varepsilon \ll 1$, and α is positive and large enough that $u = v = 0$ is the only steady state. Show that the system is excitable, and show, by means of a phase plane analysis, that solitary travelling waves of the form $u(\xi), v(\xi)$, $\xi = ct - x$, are possible with $c > 0$ and $u, v \to 0$ as $\xi \to \pm\infty$.

1.22 u and v satisfy the equations

$$\begin{aligned} \delta u_t &= \varepsilon^2 u_{xx} + f(u,v), \\ v_t &= v_{xx} + g(u,v), \end{aligned}$$

where

$$f(u,v) = u[F(u) - v], \quad g(u,v) = v[u - G(v)],$$

and $F(u)$ is a unimodal function ($F'' < 0$) with $F(0) = 0$, while $G(v)$ is monotone increasing ($G' > 0$) and $G(0) > 0$, and there is a unique point (u_0, v_0) in

[8] See Watson (1944, pp. 199 f.) for these results.

the positive quadrant where $f(u_0, v_0) = g(u_0, v_0) = 0$, and $F'(u_0) < 0$. (For example $F = u(1-u)$, $G = 0.5 + v$.)

Examine the conditions on δ and ε^2 which ensure that diffusive-driven instability of (u_0, v_0) occurs.

If the upper and lower branches of F^{-1} are denoted as $u_+(v) > u_-(v)$, explain why u_- is unstable when $\varepsilon \ll 1$. By constructing phase portraits for v when $u = 0$ and when $u = u_+(v)$, and 'gluing' them together at a fixed value $v = v^*$, show that spatially periodic solutions exist which are 'patchy', in the sense that u alternates rapidly between $u_+(v)$ and 0.